CMD®

Osaka Univ.

Possible nano-graphene device structures: A design and a simulation

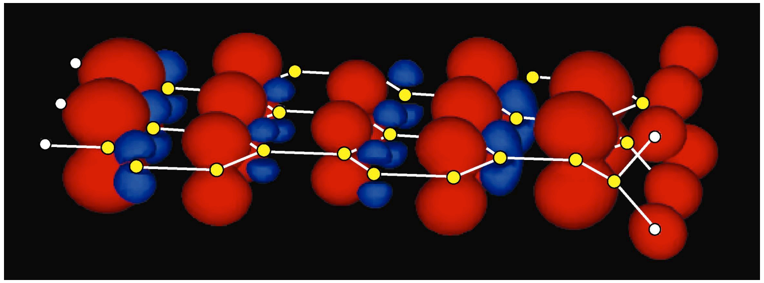

Koichi Kusakabe

The Graduate School of Engineering Science,

Osaka University,

1-3 Machikaneyama-cho, Toyonaka, Osaka 560-8531, Japan

The nano-graphite: nanoscale graphene

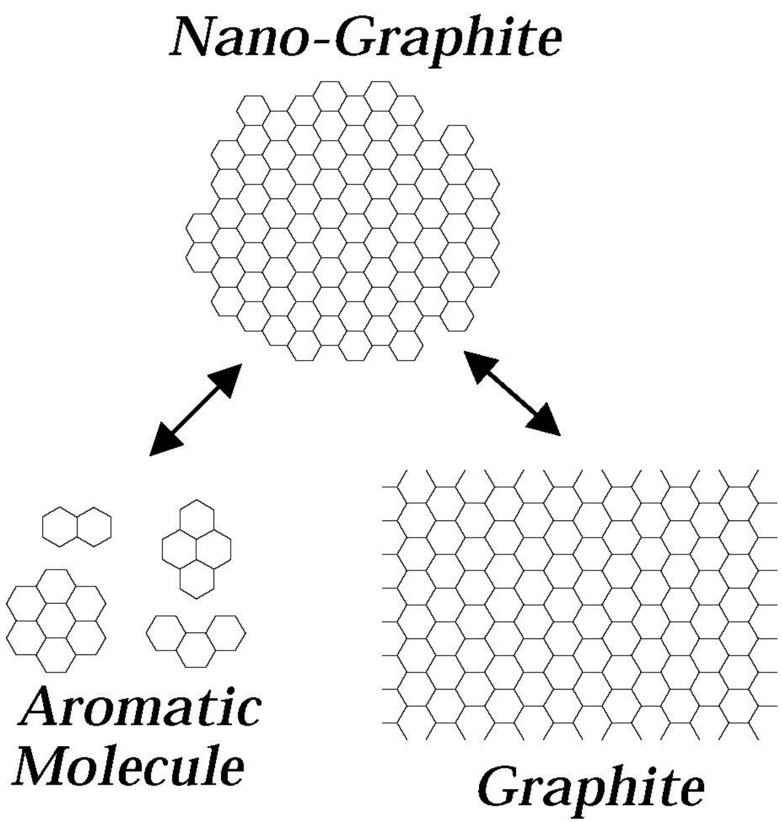

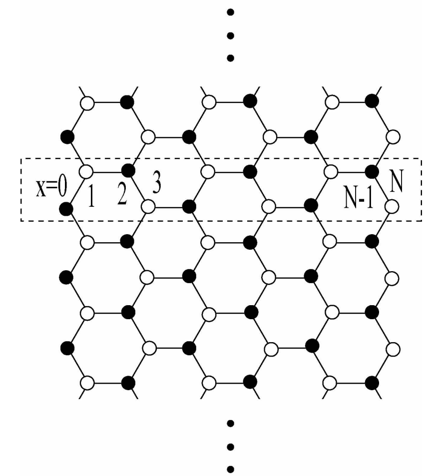

Flat bands caused by the edge states (non-bonding damping waves)

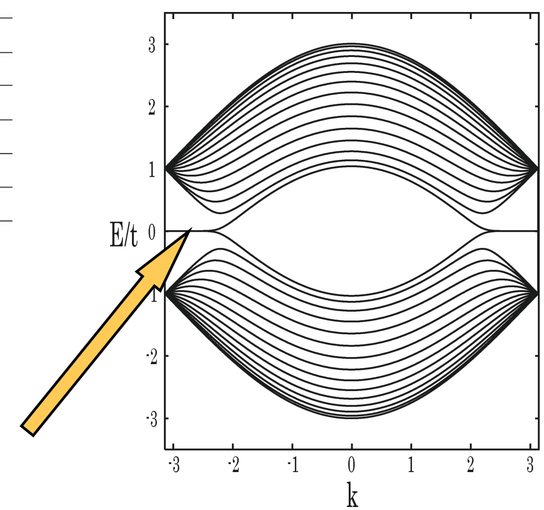

Tight-binding band structure
(π-electrons, only)

The nano-graphite: nanoscale graphene

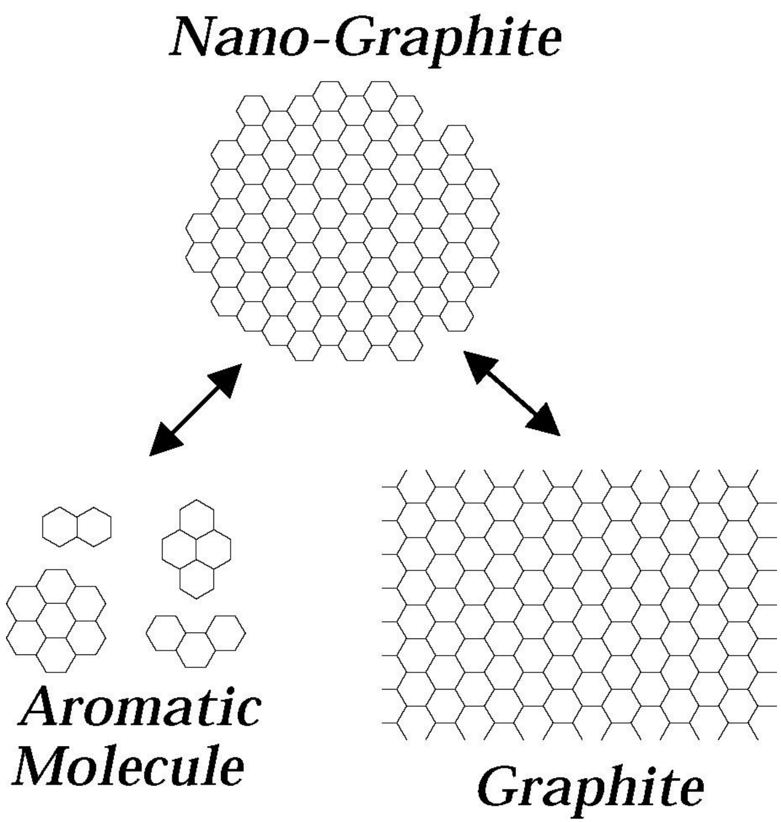

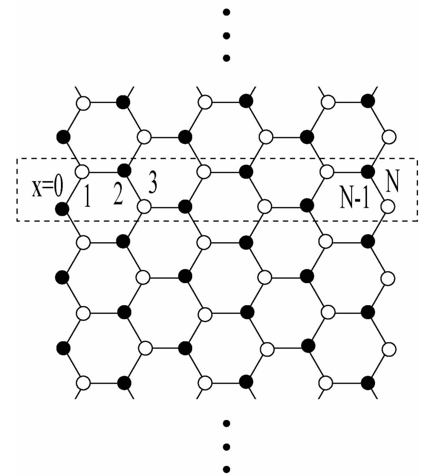

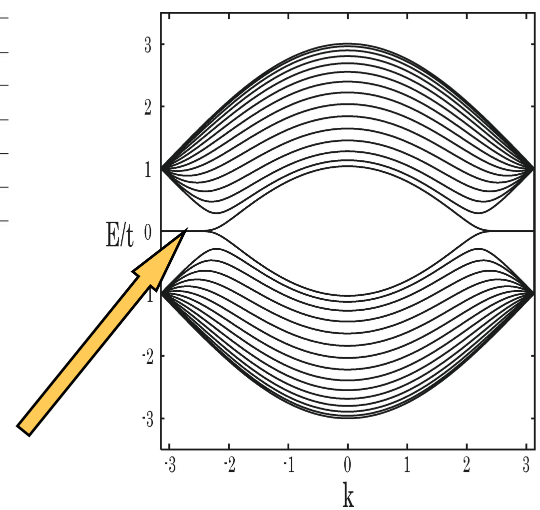

Flat bands caused by the edge states (non-bonding damping waves)

Tight-binding band structure (π-electrons, only)

Magnetic & non-magnetic edges

The DFT-LDA model tells that,

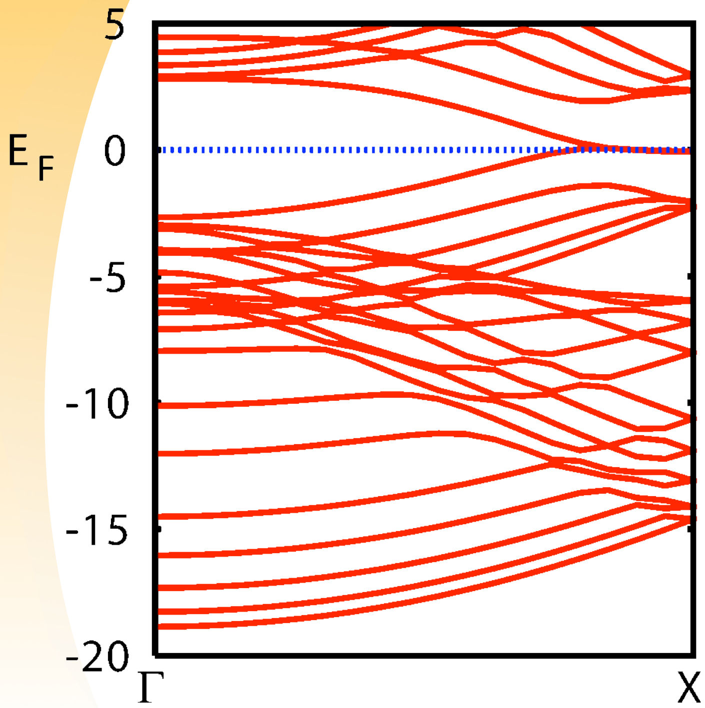

Hydrogen-terminated
zigzag nano-graphite ribbon.
Flat bands with AF spin structure,

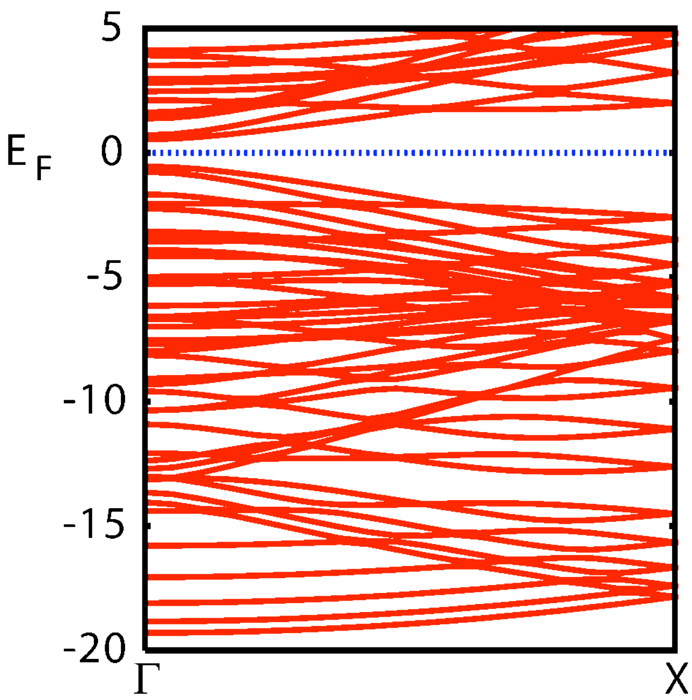

Hydrogen-terminated
armchair nano-graphite ribbon
without spin structure.

Magnetic & non-magnetic edges

The DFT-LDA model tells that,

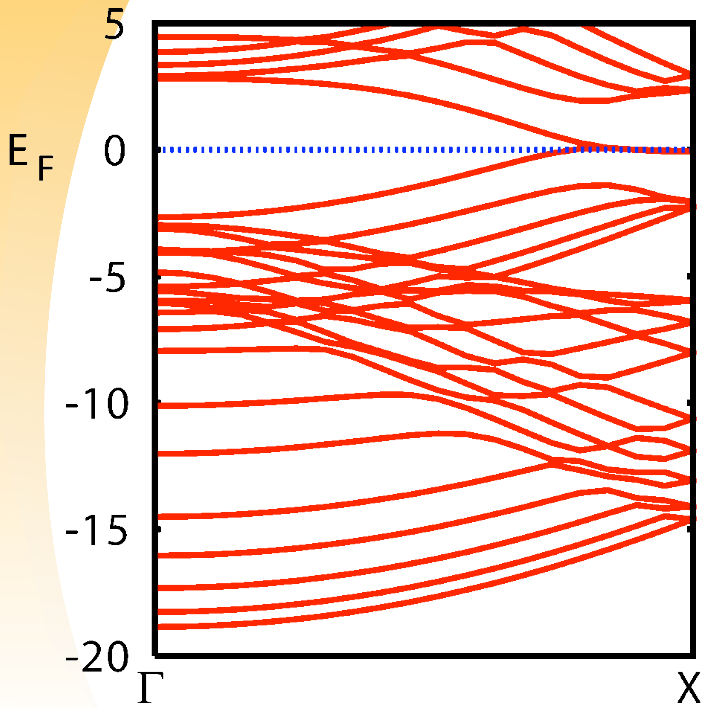

Hydrogen-terminated
zigzag nano-graphite ribbon.
Flat bands with AF spin structure,

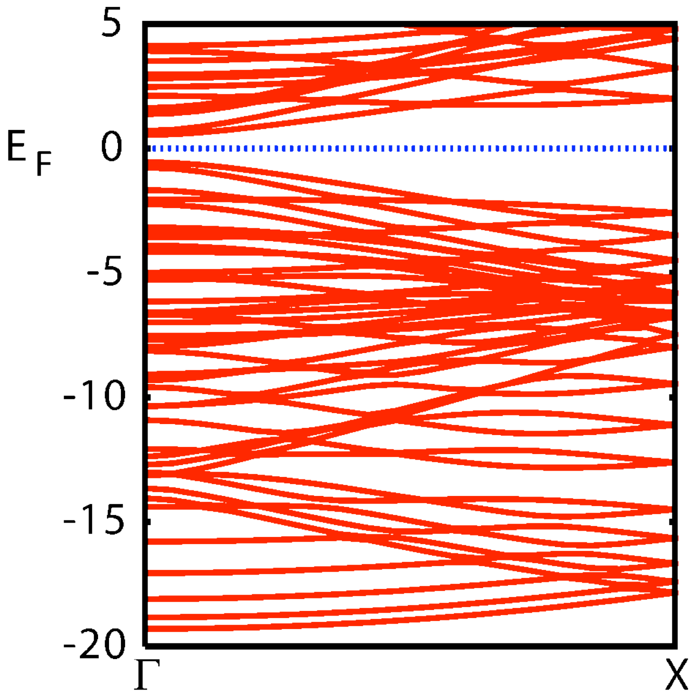

Hydrogen-terminated
armchair nano-graphite ribbon
without spin structure.

The edge states

STM & STS spectra of the zigzag edge

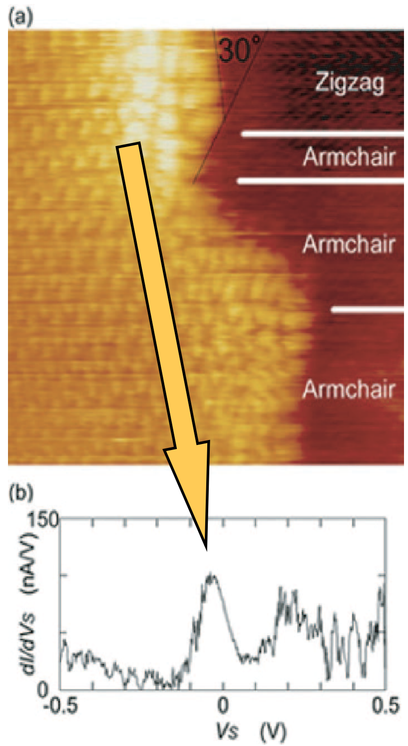

STM & STS spectra of the armchair edge

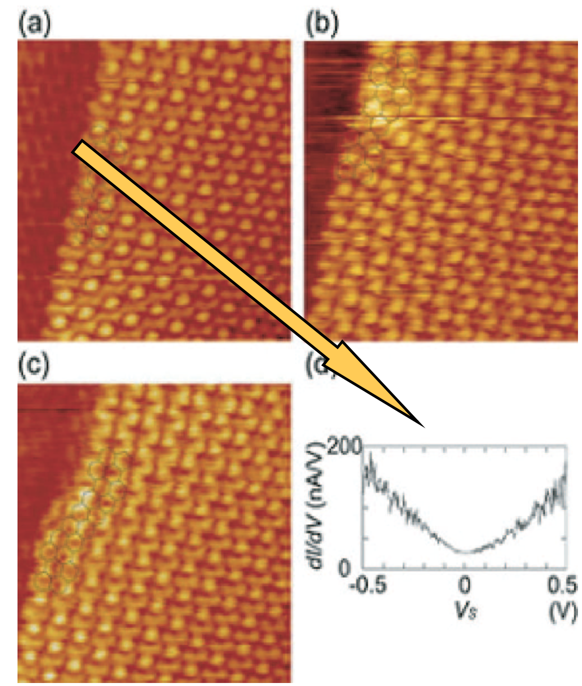

Existence of the edge state at the zigzag edge & non-existence of the state at the armchair edge are thus confirmed.

Y. Kobayashi et al., PRB 71 (2005) 193406.

Osaka Univ.
CMD®

The edge states

STM & STS spectra of the zigzag edge

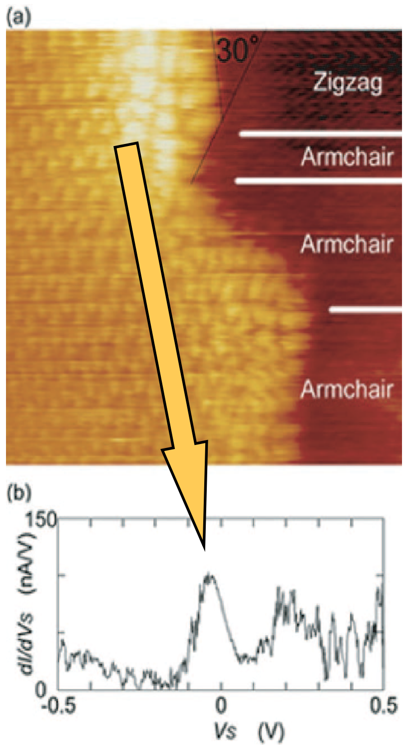

STM & STS spectra of the armchair edge

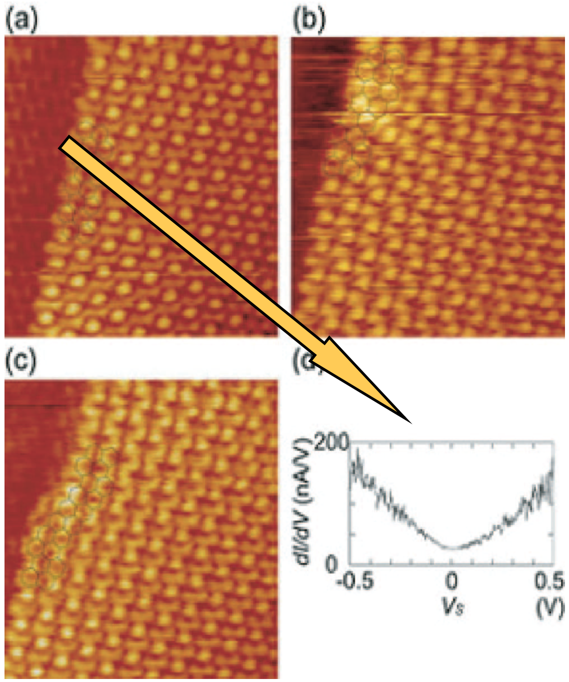

Existence of the edge state at the zigzag edge & non-existence of the state at the armchair edge are thus confirmed.

Y. Kobayashi et al., PRB 71 (2005) 193406.

Osaka Univ.
CMD®

Edge states & possible magnetism

Professor Mitsutaka Fujita
(1959-1998)

Journal of the Physical Society of Japan
Vol. 65, No. 7, July, 1996, pp. 1920-1923

LETTERS

Peculiar Localized State at Zigzag Graphite Edge

Mitsutaka FUJITA, Katsunori WAKABAYASHI, Kyoko NAKADA
and Koichi KUSAKABE[1]

Institute of Materials Science, University of Tsukuba, Tsukuba 305
[1]*Institute for Solid State Physics, University of Tokyo, Roppongi, Tokyo 106*

(Received April 30, 1996)

We study the electronic states of graphite ribbons with edges of two typical shapes, armchair and zigzag, by performing tight binding band calculations, and find that the graphite ribbons show striking contrast in the electronic states depending on the edge shape. In particular, a zigzag ribbon shows a remarkably sharp peak of density of states at the Fermi level, which does not originate from infinite graphite. We find that the singular electronic states arise from the partly flat bands at the Fermi level, whose wave functions are mainly localized on the zigzag edge. We reveal the puzzle for the emergence of the peculiar edge state by deriving the analytic form in the case of semi-infinite graphite with a zigzag edge. Applying the Hubbard model within the mean-field approximation, we discuss the possible magnetic structure in nanometer-scale micrographite.

KEYWORDS: edge state, micrographite, nanometer scale, flat band, localized state, graphite edge

The edge states, i.e. non-bonding surface states (zero modes) at the zigzag edges, may cause localized magnetism in graphitic structures, i.e. nano-graphite.

M. Fujita, K. Wakabayashi, K. Nakada, K. Kusakabe, JPSJ 65 (1996) 1920.

Edge states & possible magnetism

Professor Mitsutaka Fujita
(1959-1998)

Journal of the Physical Society of Japan
Vol. 65, No. 7, July, 1996, pp. 1920-1923 LETTERS

Peculiar Localized State at Zigzag Graphite Edge

Mitsutaka FUJITA, Katsunori WAKABAYASHI, Kyoko NAKADA
and Koichi KUSAKABE[1]

Institute of Materials Science, University of Tsukuba, Tsukuba 305
[1] *Institute for Solid State Physics, University of Tokyo, Roppongi, Tokyo 106*

(Received April 30, 1996)

We study the electronic states of graphite ribbons with edges of two typical shapes, armchair and zigzag, by performing tight binding band calculations, and find that the graphite ribbons show striking contrast in the electronic states depending on the edge shape. In particular, a zigzag ribbon shows a remarkably sharp peak of density of states at the Fermi level, which does not originate from infinite graphite. We find that the singular electronic states arise from the partly flat bands at the Fermi level, whose wave functions are mainly localized on the zigzag edge. We reveal the puzzle for the emergence of the peculiar edge state by deriving the analytic form in the case of semi-infinite graphite with a zigzag edge. Applying the Hubbard model within the mean-field approximation, we discuss the possible magnetic structure in nanometer-scale micrographite.

KEYWORDS: edge state, micrographite, nanometer scale, flat band, localized state, graphite edge

The edge states, i.e. non-bonding surface states (zero modes) at the zigzag edges, may cause localized magnetism in graphitic structures, i.e. nano-graphite.

M. Fujita, K. Wakabayashi, K. Nakada, K. Kusakabe, JPSJ 65 (1996) 1920.

Purpose of the present study

To reconfirm and to show the following issues by theoretical investigation of electron models.

- **Nano-graphene : Electronic structure is affected by the shape of edges.**
  - Non-magnetic gapped, non-magnetic metallic.
  - Anti-ferromagnetic metallic, ferrimagnetic metallic.
- **Fabrication of edges : We have possible methods to create various nano-graphene ribbon structures.**
  - Hydrogen termination, chemical modification.
  - Application of pulsed bias by the STM tip.
  - Epitaxial arrangement on surfaces & of interfaces.

Purpose of the present study

To reconfirm and to show the following issues by theoretical investigation of electron models.

- **Nano-graphene : Electronic structure is affected by the shape of edges.**
  - Non-magnetic gapped, non-magnetic metallic.
  - Anti-ferromagnetic metallic, ferrimagnetic metallic.
- **Fabrication of edges : We have possible methods to create various nano-graphene ribbon structures.**
  - Hydrogen termination, chemical modification.
  - Application of pulsed bias by the STM tip.
  - Epitaxial arrangement on surfaces & of interfaces.

Design of magnetic nano-graphite

- **Idea: Existence of flat-bands at E_F suggests magnetic instability.**
- **Strategy: π-topology**
- **Principle:**

  $|N_A - N_B| > 0 \rightarrow S > 0$

- **Supporting facts:**
  - The Longuet-Higgins rule
  - The Ovchinnikov rule
  - The Lieb theorem for the Hubbard model
  - The Shen, Qiu & Tian theorem for the ferrimagnetic RLO for the Hubbard model

The basic design

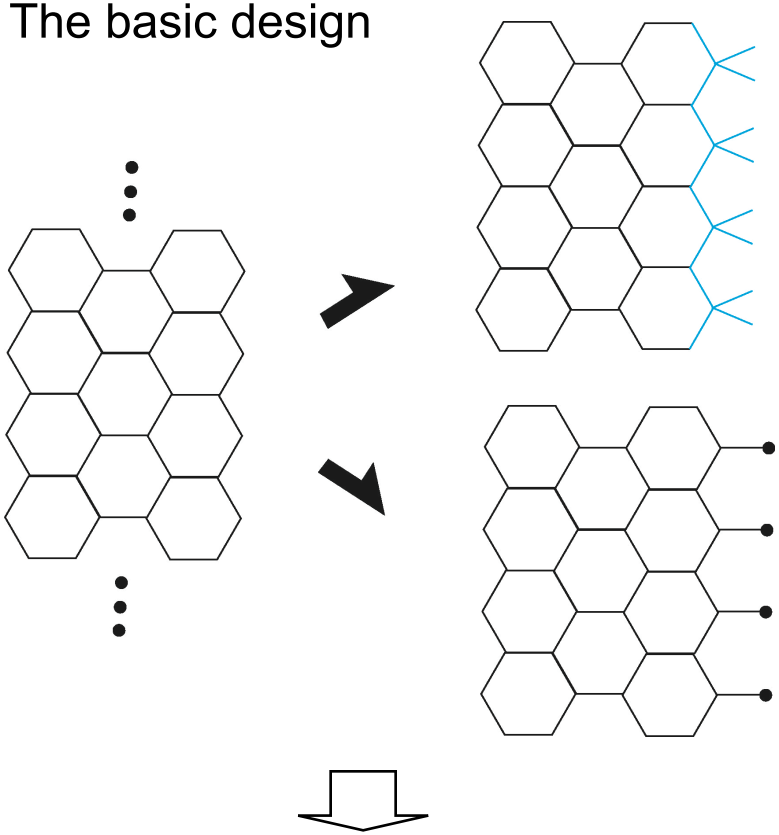

A materials solution has to be figured out.

K. Kusakabe and Y. Takagi, Mol Cryst. Liq. Cryst, 387 (2002) 231.

Design of magnetic nano-graphite

- **Idea: Existence of flat-bands at E_F suggests magnetic instability.**
- **Strategy: π-topology**
- **Principle:**

  $|N_A - N_B| > 0 \rightarrow S > 0$
- **Supporting facts:**
  - The Longuet-Higgins rule
  - The Ovchinnikov rule
  - The Lieb theorem for the Hubbard model
  - The Shen, Qiu & Tian theorem for the ferrimagnetic RLO for the Hubbard model

The basic design

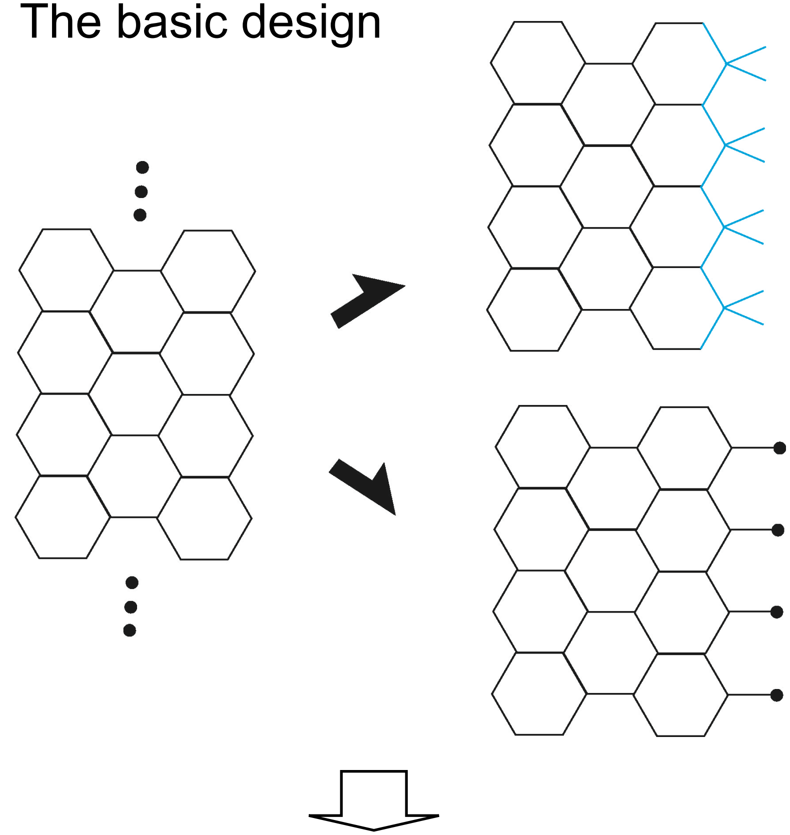

A materials solution has to be figured out.

K. Kusakabe and Y. Takagi, Mol Cryst. Liq. Cryst, 387 (2002) 231.

Step-by-step confirmation

- **All of available theoretical calculations are model calculations. We have a series of effective Hamiltonians approaching to the true Hamiltonian**
  - The tight-binding model without two-body terms
    - LCAO description
    - Non-interacting electron picture
  - The Hubbard model (the extended Hubbard model)
    - LCAO description
    - Interacting electron picture with effective interaction
  - The density-functional theory in the Kohn-Sham scheme
    - Delocalized electron picture
    - Non-interacting electron picture
  - The density-functional theory in the extended Kohn-Sham scheme (multi-reference DFT)
    - Delocalized & localized electron picture
    - Interacting electron picture with effective interaction

Effective for Materials Design ↓

Step-by-step confirmation

- **All of available theoretical calculations are model calculations. We have a series of effective Hamiltonians approaching to the true Hamiltonian**
  - The tight-binding model without two-body terms
    - LCAO description
    - Non-interacting electron picture
  - The Hubbard model (the extended Hubbard model)
    - LCAO description
    - Interacting electron picture with effective interaction
  - The density-functional theory in the Kohn-Sham scheme
    - Delocalized electron picture
    - Non-interacting electron picture
  - The density-functional theory in the extended Kohn-Sham scheme (multi-reference DFT)
    - Delocalized & localized electron picture
    - Interacting electron picture with effective interaction

Effective for Materials Design ↓

A graphene ribbon as a bipartite lattice

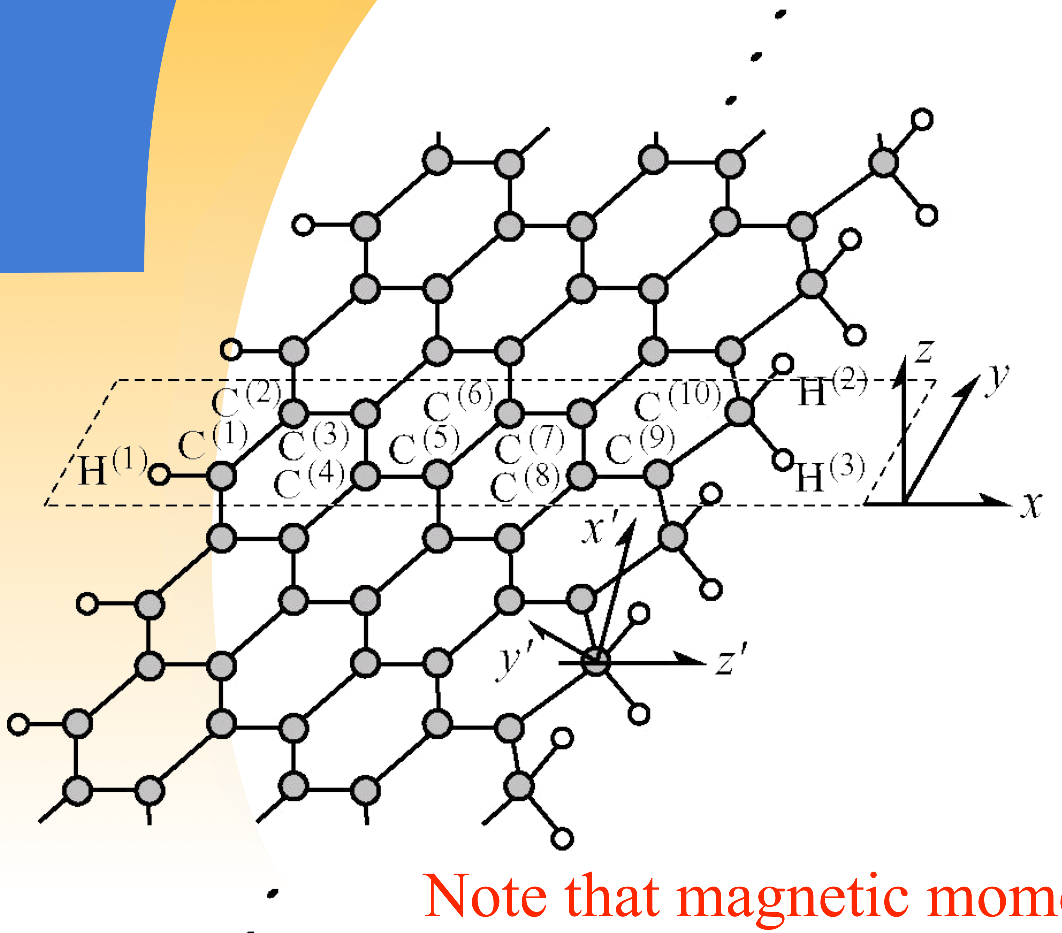

The π network on the graphene ribbon can be identified as a bipartite lattice with $|N_A\text{-}N_B|>0$.

Note that magnetic moment should appear if $|N_A\text{-}N_B|>0$. Disorder does not give a problem.

K. Kusakabe and M. Maruyama, PRB 67 (2003) 092406.

A graphene ribbon as a bipartite lattice

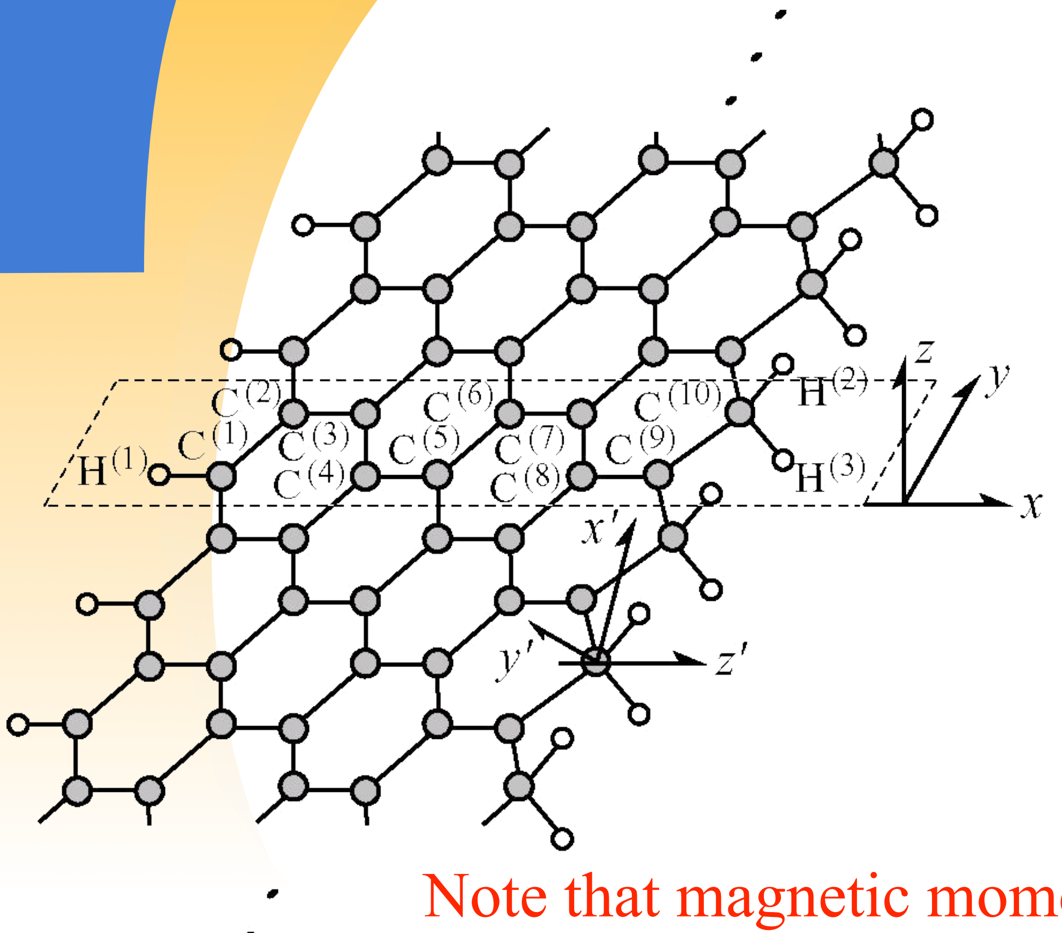

The π network on the graphene ribbon can be identified as a bipartite lattice with $|N_A - N_B| > 0$.

Note that magnetic moment should appear if $|N_A - N_B| > 0$. Disorder does not give a problem.

K. Kusakabe and M. Maruyama, PRB 67 (2003) 092406.

A flat-band Hubbard model

- Note that by making a linear combination of

$$\phi_1 = \phi_s + \phi_{x'} + \phi_{y'} + \phi_{z'}$$
$$\phi_2 = \phi_s - \phi_{x'} - \phi_{y'} + \phi_{z'}.$$

pointing to H$^{(2)}$ and H$^{(3)}$, we have

$$\bar{\phi}_- = (\phi_1 - \phi_2)/\sqrt{2} = \phi_z.$$

- Utilizing $\bar{\phi}_-$, a linear combination of 1s orbitals $\bar{\varphi}_- = (\varphi_1 - \varphi_2)/\sqrt{2}$ as well as the π orbitals on C$^{(i)}$ $(i = 1, \cdots 9)$, we obtain an effective Hamiltonian.

$$\begin{aligned} H &= -\sum_{\langle i,j\rangle}\sum_{\sigma} t_{i,j}(c^\dagger_{i,\sigma}c_{j,\sigma} + H.c.) + \sum_i U n_{i,\uparrow}n_{i,\downarrow} \\ &\quad -\sum_{\langle i,l\rangle}\sum_{\sigma} t'_{i,l}(c^\dagger_{i,\sigma}d_{l,\sigma} + H.c.) + \sum_l U' m_{l,\uparrow}m_{l,\downarrow} \\ &\quad +\varepsilon \sum_l \sum_\sigma m_{l,\sigma} \qquad (1) \end{aligned}$$

- If $\varepsilon = \varepsilon_{1s} - \varepsilon_{2p} = 0$ and if $U' = U$, the Lieb theorem is applicable.

A flat-band Hubbard model

- Note that by making a linear combination of

$$\phi_1 = \phi_s + \phi_{x'} + \phi_{y'} + \phi_{z'}$$
$$\phi_2 = \phi_s - \phi_{x'} - \phi_{y'} + \phi_{z'}.$$

pointing to $H^{(2)}$ and $H^{(3)}$, we have

$$\bar{\phi}_- = (\phi_1 - \phi_2)/\sqrt{2} = \phi_z.$$

- Utilizing $\bar{\phi}_-$, a linear combination of 1s orbitals $\bar{\varphi}_- = (\varphi_1 - \varphi_2)/\sqrt{2}$ as well as the π orbitals on $C^{(i)}$ $(i = 1, \cdots 9)$, we obtain an effective Hamiltonian.

$$\begin{aligned} H = & - \sum_{\langle i,j \rangle} \sum_{\sigma} t_{i,j} (c^\dagger_{i,\sigma} c_{j,\sigma} + H.c.) + \sum_i U n_{i,\uparrow} n_{i,\downarrow} \\ & - \sum_{\langle i,l \rangle} \sum_{\sigma} t'_{i,l} (c^\dagger_{i,\sigma} d_{l,\sigma} + H.c.) + \sum_l U' m_{l,\uparrow} m_{l,\downarrow} \\ & + \varepsilon \sum_l \sum_\sigma m_{l,\sigma} \qquad (1) \end{aligned}$$

- If $\varepsilon = \varepsilon_{1s} - \varepsilon_{2p} = 0$ and if $U' = U$, the Lieb theorem is applicable.

A flat-band Hubbard model

- Note that by making a linear combination of

$$\phi_1 = \phi_s + \phi_{x'} + \phi_{y'} + \phi_{z'}$$
$$\phi_2 = \phi_s - \phi_{x'} - \phi_{y'} + \phi_{z'}.$$

pointing to $H^{(2)}$ and $H^{(3)}$, we have

$$\bar{\phi}_- = (\phi_1 - \phi_2)/\sqrt{2} = \phi_z.$$

- Utilizing $\bar{\phi}_-$, a linear combination of 1s orbitals $\bar{\varphi}_- = (\varphi_1 - \varphi_2)/\sqrt{2}$ as well as the π orbitals on $C^{(i)}$ $(i = 1, \cdots 9)$, we obtain an effective Hamiltonian.

$$\begin{aligned} H &= -\sum_{\langle i,j\rangle}\sum_{\sigma} t_{i,j}(c^\dagger_{i,\sigma}c_{j,\sigma} + H.c.) + \sum_i U n_{i,\uparrow}n_{i,\downarrow} \\ &\quad -\sum_{\langle i,l\rangle}\sum_{\sigma} t'_{i,l}(c^\dagger_{i,\sigma}d_{l,\sigma} + H.c.) + \sum_l U' m_{l,\uparrow}m_{l,\downarrow} \\ &\quad +\varepsilon\sum_l\sum_\sigma m_{l,\sigma} \qquad (1) \end{aligned}$$

- If $\varepsilon = \varepsilon_{1s} - \varepsilon_{2p} = 0$ and if $U' = U$, the Lieb theorem is applicable.

The electronic band-structure calculation

A flat-band Hubbard model

- Note that by making a linear combination of

$$\phi_1 = \phi_s + \phi_{x'} + \phi_{y'} + \phi_{z'}$$
$$\phi_2 = \phi_s - \phi_{x'} - \phi_{y'} + \phi_{z'}.$$

pointing to $H^{(2)}$ and $H^{(3)}$, we have

$$\bar{\phi}_- = (\phi_1 - \phi_2)/\sqrt{2} = \phi_z.$$

- Utilizing $\bar{\phi}_-$, a linear combination of 1s orbitals $\bar{\varphi}_- = (\varphi_1 - \varphi_2)/\sqrt{2}$ as well as the π orbitals on $C^{(i)}$ $(i = 1, \cdots 9)$, we obtain an effective Hamiltonian.

$$\begin{aligned} H &= -\sum_{\langle i,j \rangle}\sum_{\sigma} t_{i,j}(c^{\dagger}_{i,\sigma}c_{j,\sigma} + H.c.) + \sum_i U n_{i,\uparrow}n_{i,\downarrow} \\ &\quad -\sum_{\langle i,l \rangle}\sum_{\sigma} t'_{i,l}(c^{\dagger}_{i,\sigma}d_{l,\sigma} + H.c.) + \sum_l U' m_{l,\uparrow}m_{l,\downarrow} \\ &\quad +\varepsilon\sum_l\sum_{\sigma} m_{l,\sigma} \qquad (1) \end{aligned}$$

- If $\varepsilon = \varepsilon_{1s} - \varepsilon_{2p} = 0$ and if $U' = U$, the Lieb theorem is applicable.

The electronic band-structure calculation

A flat-band Hubbard model

- Note that by making a linear combination of

$$\phi_1 = \phi_s + \phi_{x'} + \phi_{y'} + \phi_{z'}$$
$$\phi_2 = \phi_s - \phi_{x'} - \phi_{y'} + \phi_{z'}.$$

pointing to H$^{(2)}$ and H$^{(3)}$, we have

$$\bar{\phi}_- = (\phi_1 - \phi_2)/\sqrt{2} = \phi_z.$$

- Utilizing $\bar{\phi}_-$, a linear combination of 1s orbitals $\bar{\varphi}_- = (\varphi_1 - \varphi_2)/\sqrt{2}$ as well as the π orbitals on C$^{(i)}$ $(i = 1, \cdots 9)$, we obtain an effective Hamiltonian.

$$\begin{aligned} H &= -\sum_{\langle i,j \rangle} \sum_{\sigma} t_{i,j}(c^{\dagger}_{i,\sigma} c_{j,\sigma} + H.c.) + \sum_i U n_{i,\uparrow} n_{i,\downarrow} \\ &\quad - \sum_{\langle i,l \rangle} \sum_{\sigma} t'_{i,l}(c^{\dagger}_{i,\sigma} d_{l,\sigma} + H.c.) + \sum_l U' m_{l,\uparrow} m_{l,\downarrow} \\ &\quad + \varepsilon \sum_l \sum_{\sigma} m_{l,\sigma} \end{aligned} \qquad (1)$$

- If $\varepsilon = \varepsilon_{1s} - \varepsilon_{2p} = 0$ and if $U' = U$, the Lieb theorem is applicable.

The electronic band-structure calculation

↓

An effective many-body model
(The Hubbard model)

A flat-band Hubbard model

- Note that by making a linear combination of

$$\phi_1 = \phi_s + \phi_{x'} + \phi_{y'} + \phi_{z'}$$
$$\phi_2 = \phi_s - \phi_{x'} - \phi_{y'} + \phi_{z'}.$$

pointing to $\mathrm{H}^{(2)}$ and $\mathrm{H}^{(3)}$, we have

$$\bar{\phi}_- = (\phi_1 - \phi_2)/\sqrt{2} = \phi_z.$$

- Utilizing $\bar{\phi}_-$, a linear combination of 1s orbitals $\bar{\varphi}_- = (\varphi_1 - \varphi_2)/\sqrt{2}$ as well as the π orbitals on $\mathrm{C}^{(i)}$ $(i = 1, \cdots 9)$, we obtain an effective Hamiltonian.

$$\begin{aligned} H &= -\sum_{\langle i,j\rangle}\sum_{\sigma} t_{i,j}(c^\dagger_{i,\sigma}c_{j,\sigma} + H.c.) + \sum_i U n_{i,\uparrow}n_{i,\downarrow} \\ &\quad -\sum_{\langle i,l\rangle}\sum_{\sigma} t'_{i,l}(c^\dagger_{i,\sigma}d_{l,\sigma} + H.c.) + \sum_l U' m_{l,\uparrow}m_{l,\downarrow} \\ &\quad +\varepsilon\sum_l\sum_\sigma m_{l,\sigma} \qquad (1) \end{aligned}$$

- If $\varepsilon = \varepsilon_{1s} - \varepsilon_{2p} = 0$ and if $U' = U$, the Lieb theorem is applicable.

The electronic band-structure calculation

↓

An effective many-body model (The Hubbard model)

↓

A flat-band Hubbard model

- Note that by making a linear combination of

$$\phi_1 = \phi_s + \phi_{x'} + \phi_{y'} + \phi_{z'}$$
$$\phi_2 = \phi_s - \phi_{x'} - \phi_{y'} + \phi_{z'}.$$

pointing to $H^{(2)}$ and $H^{(3)}$, we have

$$\bar{\phi}_- = (\phi_1 - \phi_2)/\sqrt{2} = \phi_z.$$

- Utilizing $\bar{\phi}_-$, a linear combination of 1s orbitals $\bar{\varphi}_- = (\varphi_1 - \varphi_2)/\sqrt{2}$ as well as the π orbitals on $C^{(i)}$ $(i = 1, \cdots 9)$, we obtain an effective Hamiltonian.

$$\begin{aligned} H &= -\sum_{\langle i,j\rangle}\sum_{\sigma} t_{i,j}(c^\dagger_{i,\sigma}c_{j,\sigma} + H.c.) + \sum_i U n_{i,\uparrow}n_{i,\downarrow} \\ &\quad - \sum_{\langle i,l\rangle}\sum_{\sigma} t'_{i,l}(c^\dagger_{i,\sigma}d_{l,\sigma} + H.c.) + \sum_l U' m_{l,\uparrow}m_{l,\downarrow} \\ &\quad + \varepsilon\sum_l\sum_{\sigma} m_{l,\sigma} \end{aligned} \tag{1}$$

- If $\varepsilon = \varepsilon_{1s} - \varepsilon_{2p} = 0$ and if $U' = U$, the Lieb theorem is applicable.

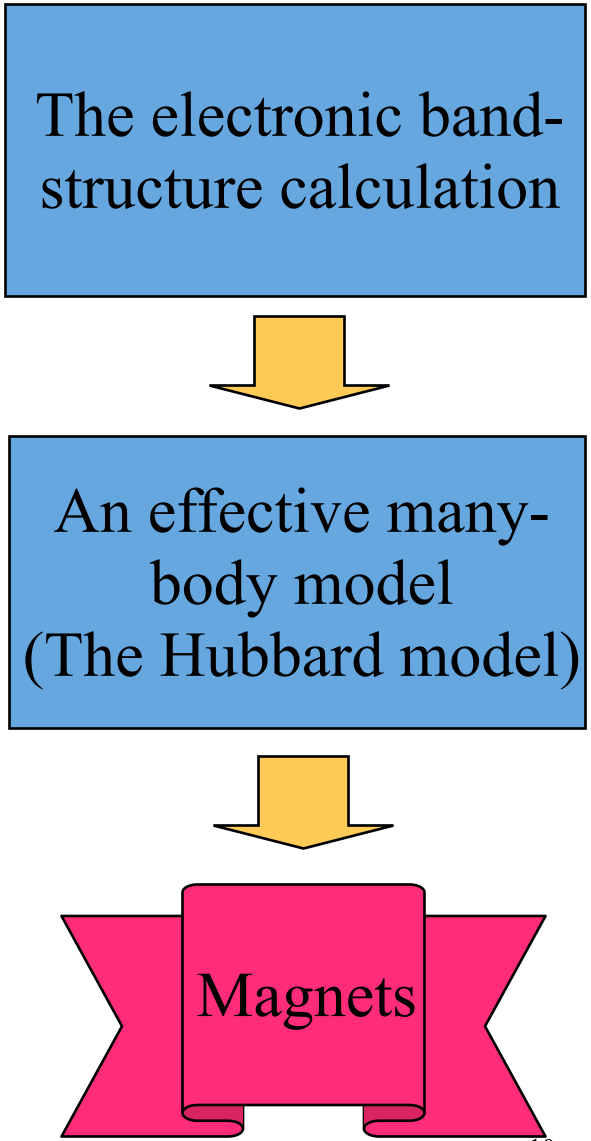

Possible materials solutions

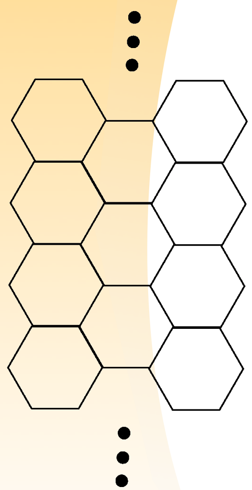

Zigzag-edged graphene ribbon

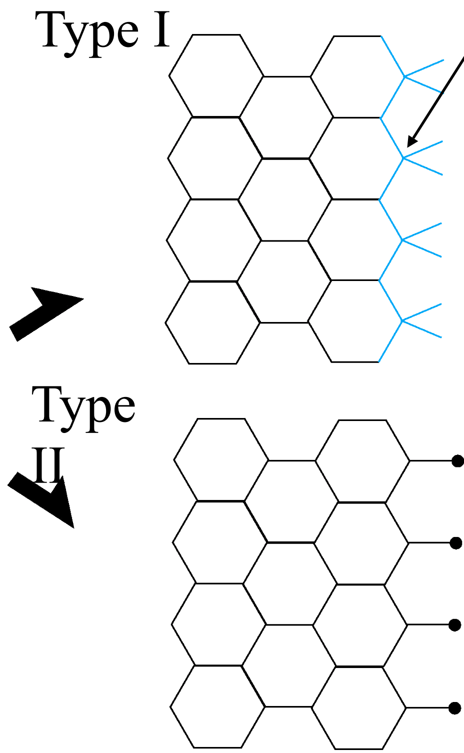

Magnetic nano-graphite ribbons

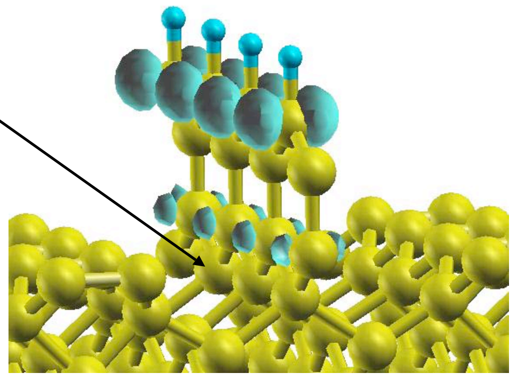

Graphite-diamond hybrid structures
K. Kusakabe, et al. (2004).

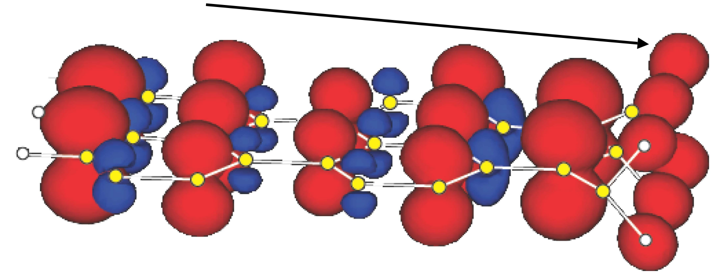

Hydrogenated nano-graphite ribbons
K. Kusakabe & M. Maruyama (2003).

Possible materials solutions

sp^3 carbon

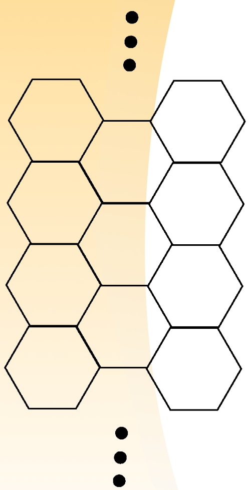

Zigzag-edged graphene ribbon

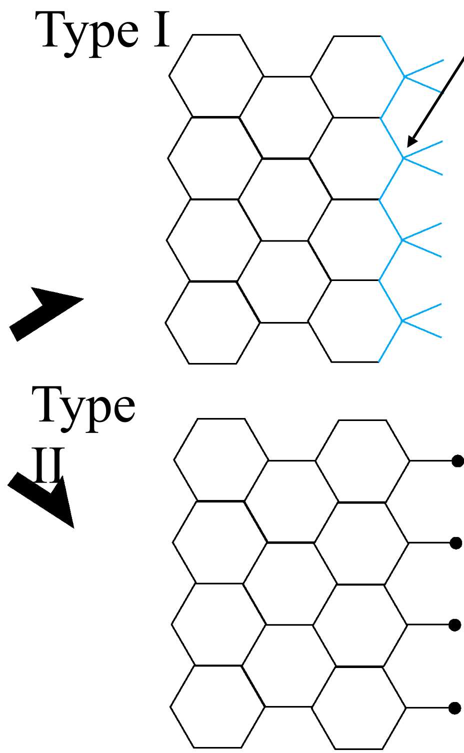

Magnetic nano-graphite ribbons

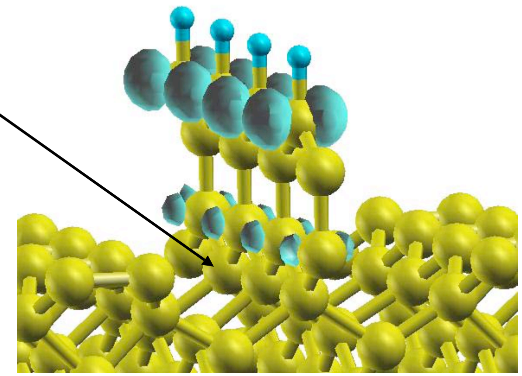

Graphite-diamond hybrid structures
K. Kusakabe, et al. (2004).

H_2 gives a π state.

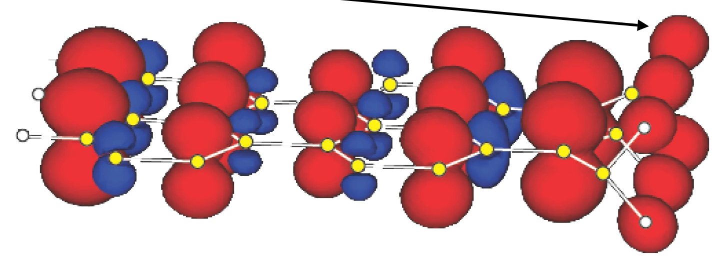

Hydrogenated nano-graphite ribbons
K. Kusakabe & M. Maruyama (2003).

A hydrogenated magnetic ribbon

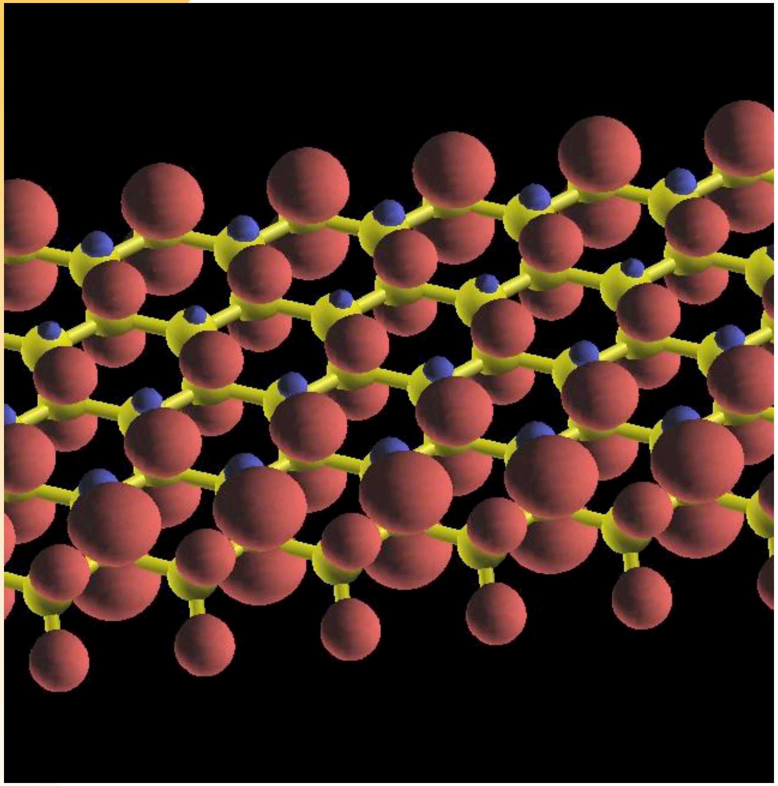

LSDA calculation of the magnetic nanographite ribbon with mono- & di-hydrogenated zigzag edges (Isosurfaces represent spin density)

K. Kusakabe and M. Maruyama, PRB 67 (2003) 092406.

A hydrogenated magnetic ribbon

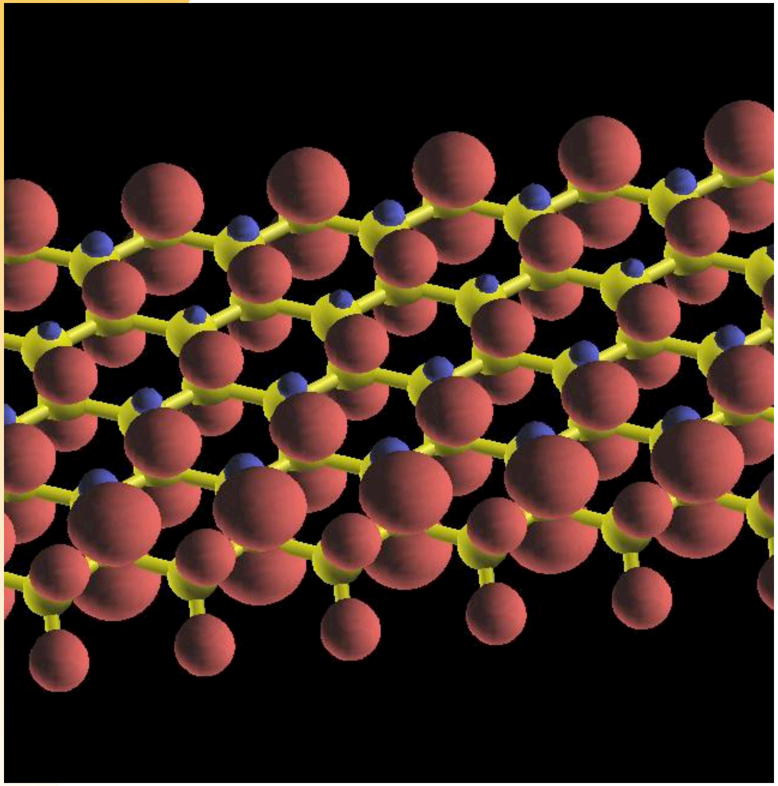

LSDA calculation of the magnetic nanographite ribbon with mono- & di-hydrogenated zigzag edges (Isosurfaces represent spin density)

K. Kusakabe and M. Maruyama, PRB 67 (2003) 092406.

A hydrogenated magnetic ribbon

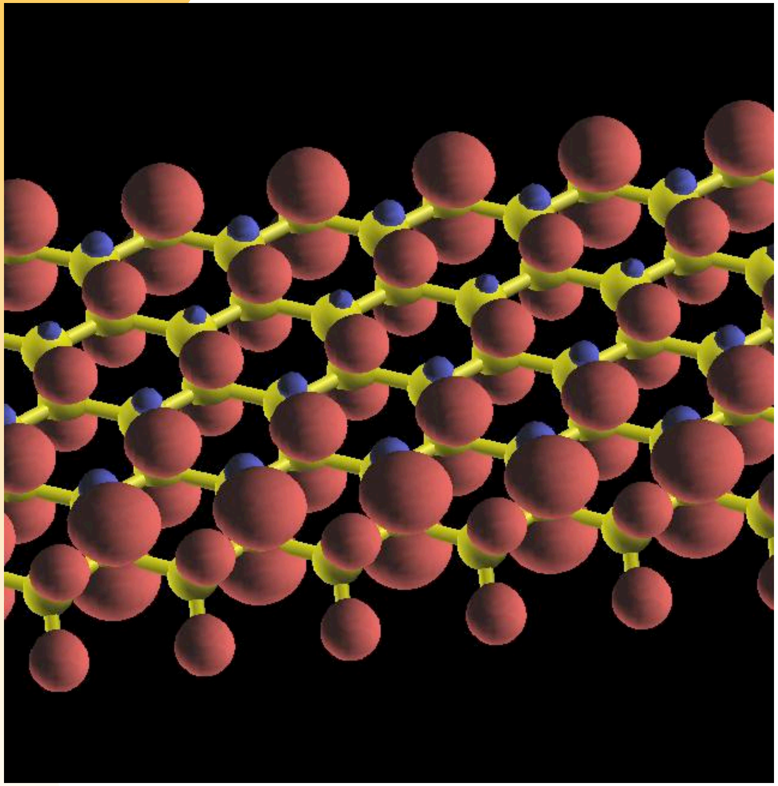

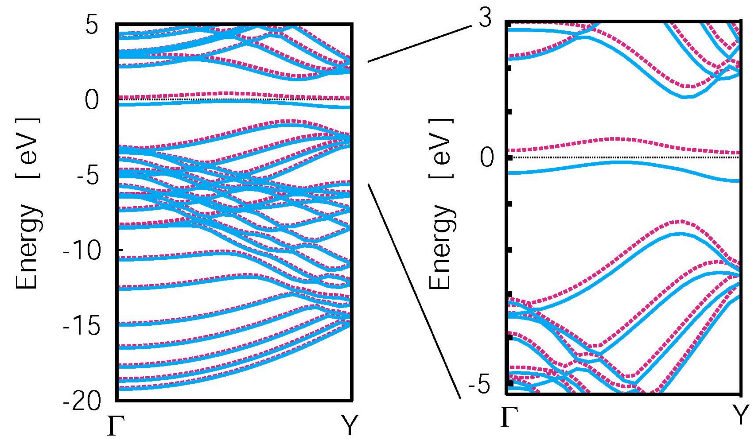

LSDA calculation of the magnetic nanographite ribbon with mono- & di-hydrogenated zigzag edges (Isosurfaces represent spin density)

K. Kusakabe and M. Maruyama, PRB 67 (2003) 092406.

Osaka Univ.
CMD®

A hydrogenated magnetic ribbon

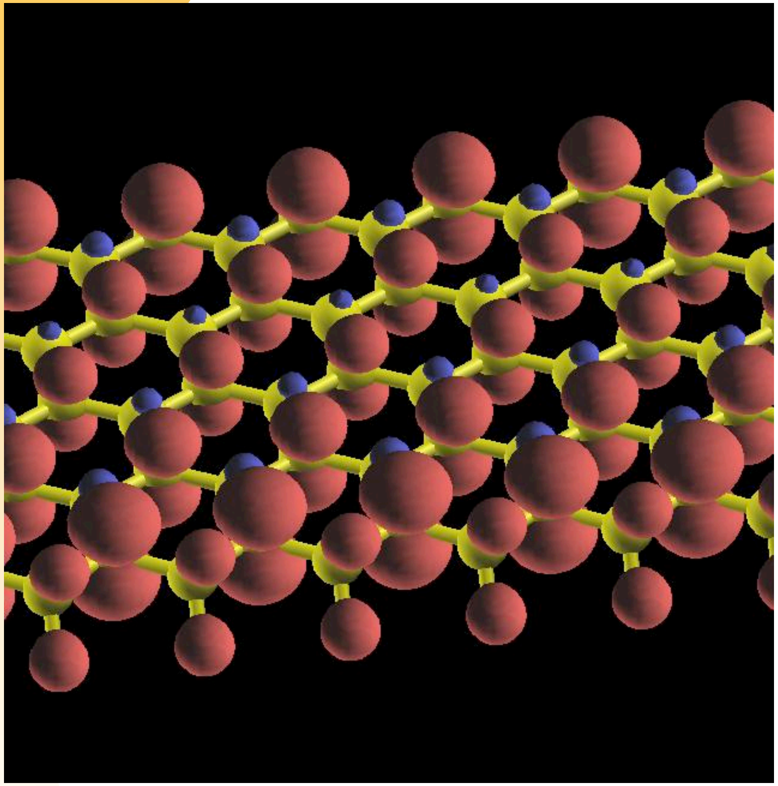

LSDA calculation of the magnetic nanographite ribbon with mono- & di-hydrogenated zigzag edges (Isosurfaces represent spin density)

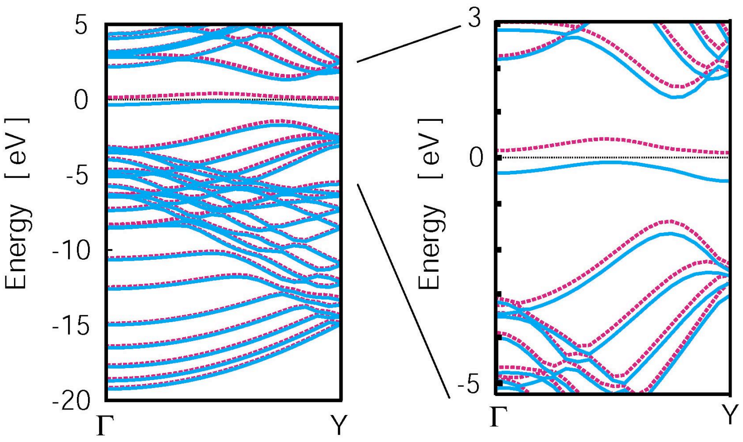

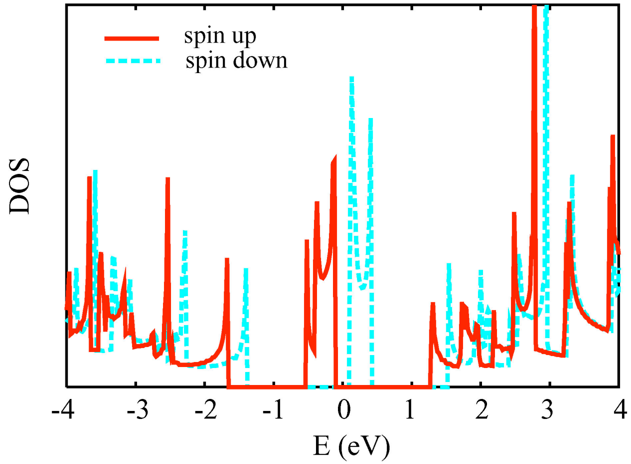

DOS of the magnetic graphene ribbon

K. Kusakabe and M. Maruyama, PRB 67 (2003) 092406.

Osaka Univ.
CMD®

Confirmation within DFT & HF

- **The magnetic nano-graphene ribbon with a mono-hydrogenated edge and a di-hydrogenated edge is confirmed to have ferrimagnetic spin alignment in 0 temperature by,**
  - LSDA calculation, GGA calculation
  - PP-PS calculation PAW calculation
  - TAPP, VASP
- **A magnetic molecule, C14H13 (1,8,9-di-hydro-anthracene) has S=3/2 confirmed by,**
  - LSDA calculation
  - URHF calculation

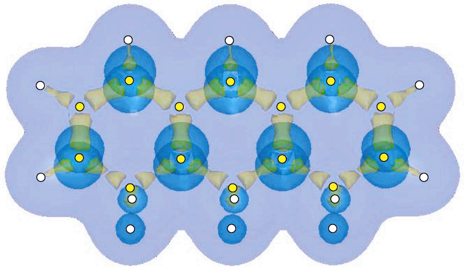

By K. Akagi.

Osaka Univ.
CMD®

Confirmation within DFT & HF

- **The magnetic nano-graphene ribbon with a mono-hydrogenated edge and a di-hydrogenated edge is confirmed to have ferrimagnetic spin alignment in 0 temperature by,**
  - LSDA calculation, GGA calculation
  - PP-PS calculation PAW calculation
  - TAPP, VASP
- **A magnetic molecule, $C14H13$ (1,8,9-di-hydro-anthracene) has S=3/2 confirmed by,**
  - LSDA calculation
  - URHF calculation

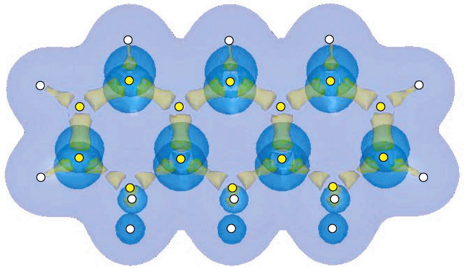

By K. Akagi.

A stable graphite-diamond hybrid structure

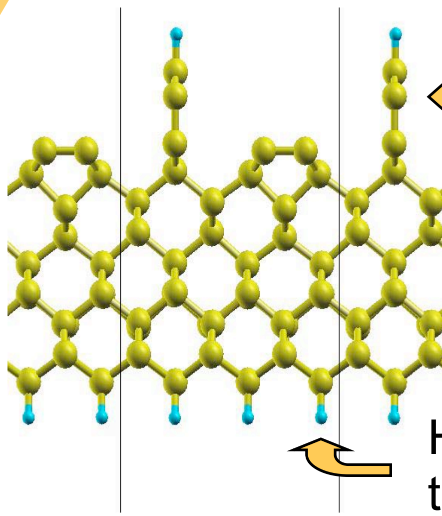

Graphene structure

A unit cell of the structure (indicated by solid lines)

Hydrogen terminated

Spin density (blue isosurfaces) in the graphite-diamond hybrid

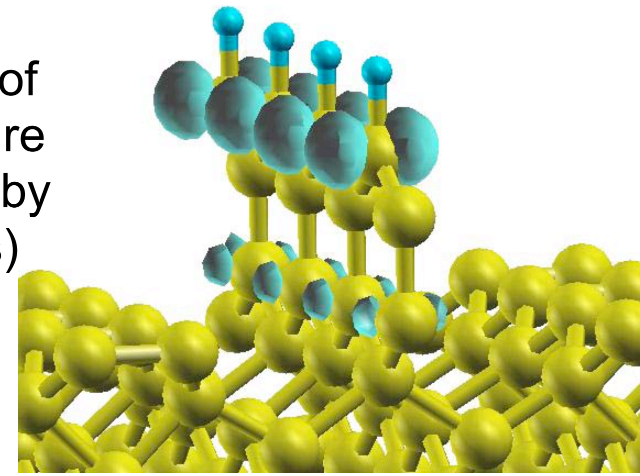

- **k-points on (6,6,1) mesh**
- **Structures are optimized.**
- **Graphene structures on 8-carbon layers in a (3×2) unit cell.**

- **S=1 (per unit cell). The moment of 1μ_B per each edge carbon atom.**
- **Spins exist only on graphitic structure.**
- **Symmetric dimers are created.**

K. Kusakabe and N. Suzuki, CP772, Physics of Semiconductors: 27th Int. Conf. Phys. Semicon. Part B 1359 (2004)

Osaka Univ.
CMD®

A stable graphite-diamond hybrid structure

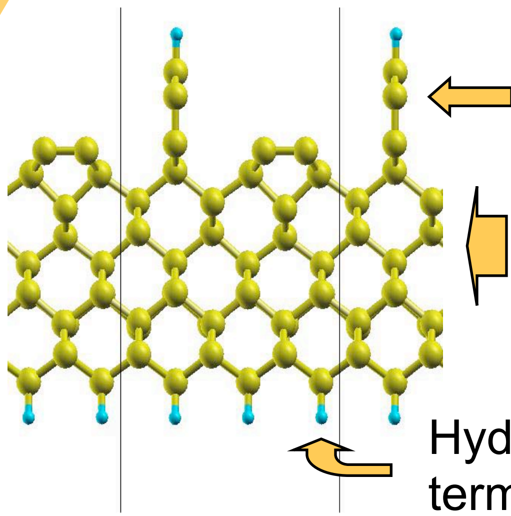

Spin density (blue isosurfaces) in the graphite-diamond hybrid

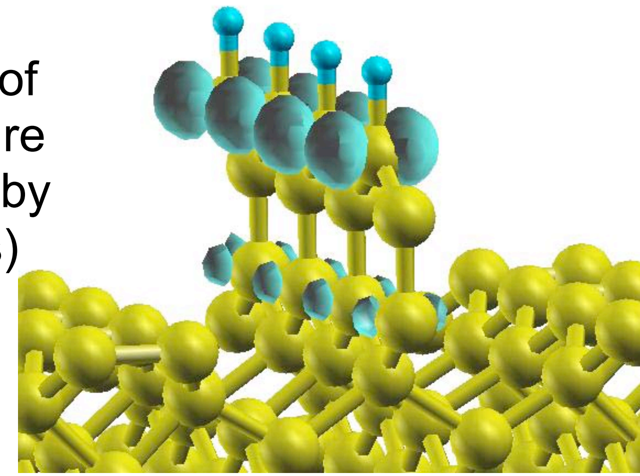

- **k-points on (6,6,1) mesh**
- **Structures are optimized.**
- **Graphene structures on 8-carbon layers in a (3×2) unit cell.**

- **S=1 (per unit cell). The moment of 1μ_B per each edge carbon atom.**
- **Spins exist only on graphitic structure.**
- **Symmetric dimers are created.**

K. Kusakabe and N. Suzuki, CP772, Physics of Semiconductors: 27th Int. Conf. Phys. Semicon. Part B 1359 (2004)

Band structure of the structure C

- **Electronic band structure for the structure has a surface π-band due to the graphene ribbon.**
- **The band (folded in the right figure due to a doubled unit cell) near E_F is strongly spin polarized. This nearly flat band consists of edge states.**
- **The band gap is ～240 meV.**
- **E_F may be shifted by applied gate voltage or by electron (or hole) doping.**

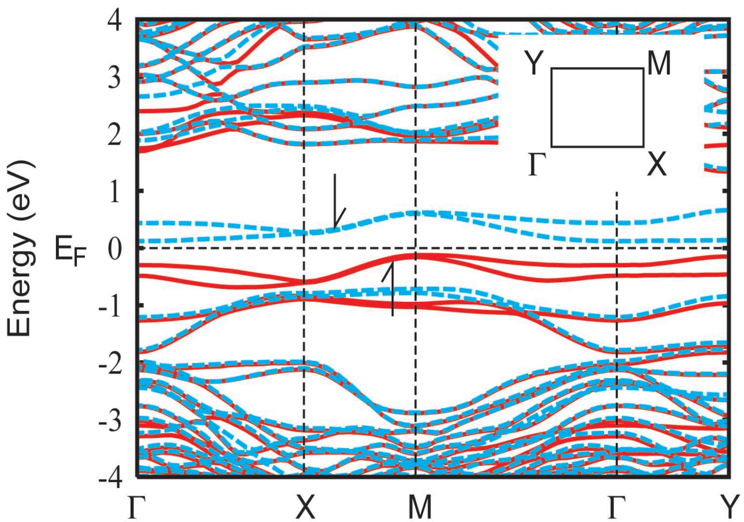

Electronic band structure of the graphite-diamond hybrid structure on a diamond (100) surface (the structure C).

Shen's theorem for the ferrimagnetism is applicable, if the π system of the ribbon is described by the Hubbard model.

Half-metallic nano wires may be created using the graphite-diamond hybrid.

Band structure of the structure C

- Electronic band structure for the structure has a surface π-band due to the graphene ribbon.
- The band (folded in the right figure due to a doubled unit cell) near E_F is strongly spin polarized. This nearly flat band consists of edge states.
- The band gap is ～240 meV.
- E_F may be shifted by applied gate voltage or by electron (or hole) doping.

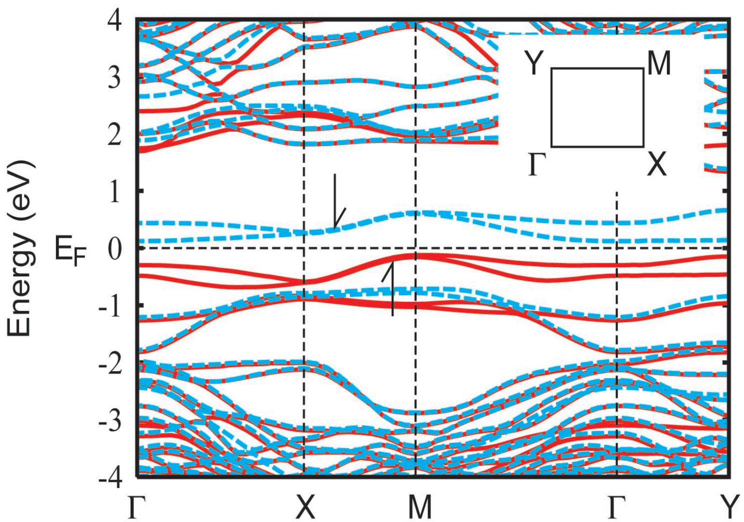

Electronic band structure of the graphite-diamond hybrid structure on a diamond (100) surface (the structure C).

Shen's theorem for the ferrimagnetism is applicable, if the π system of the ribbon is described by the Hubbard model.

→ Half-metallic nano wires may be created using the graphite-diamond hybrid.

Manufacturing Magnetic Nanographite

- The armchair edge is stable.
- Removal of odd-numbers carbon atoms would make magnetic moments.

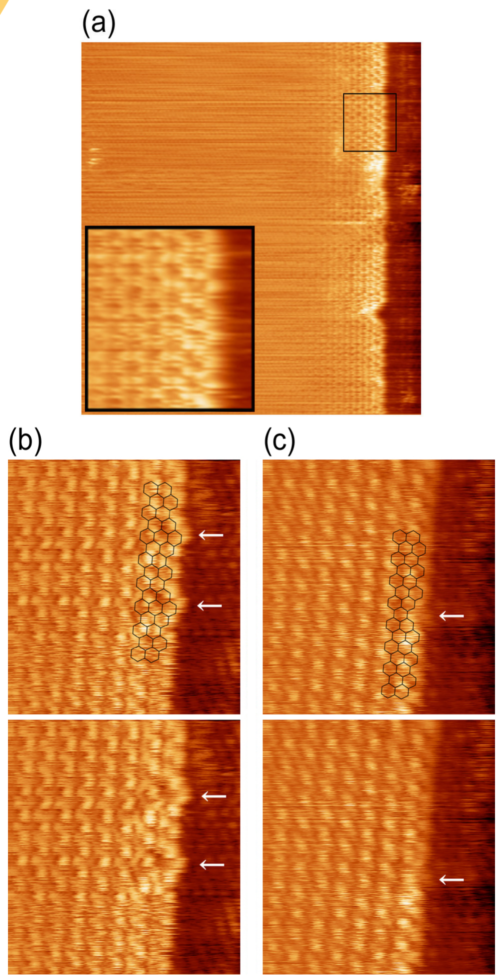

Y. Kobayashi et al. (2005).

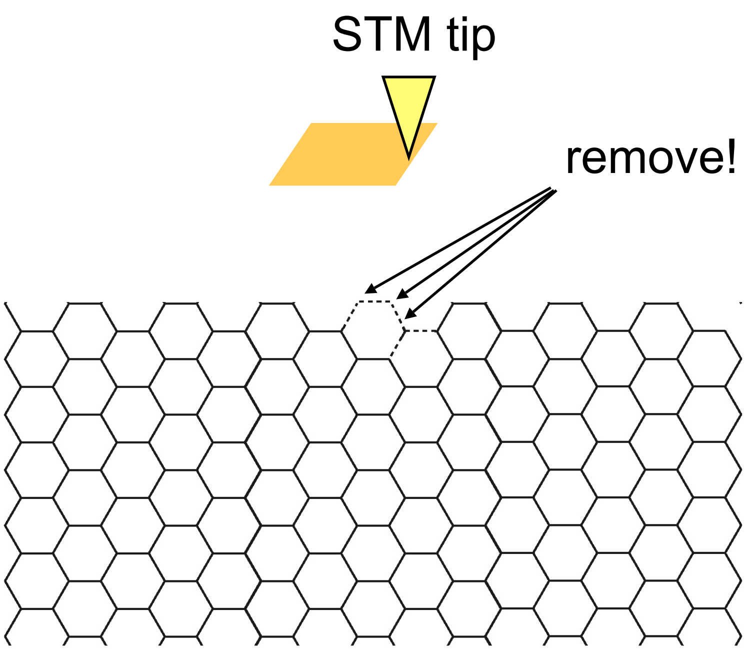

Manufacturing Magnetic Nanographite

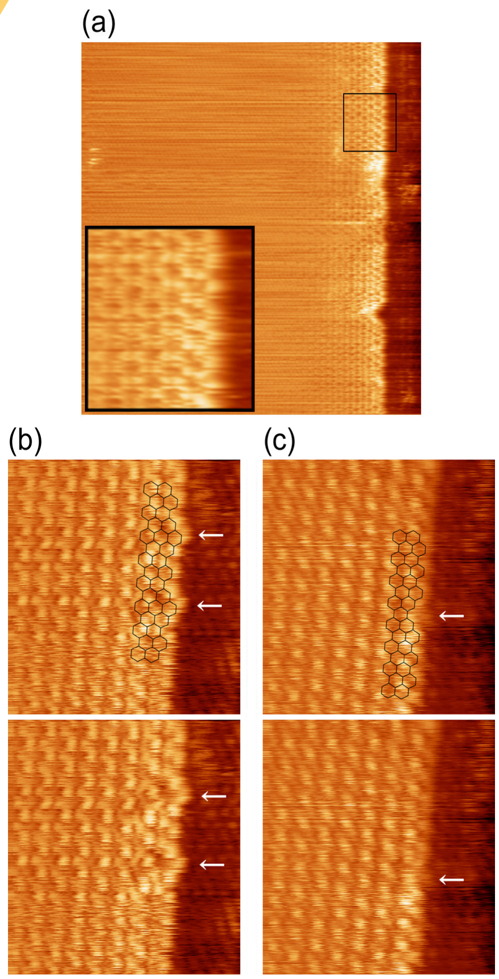

Y. Kobayashi et al. (2005).

- The armchair edge is stable.
- Removal of odd-numbers carbon atoms would make magnetic moments.

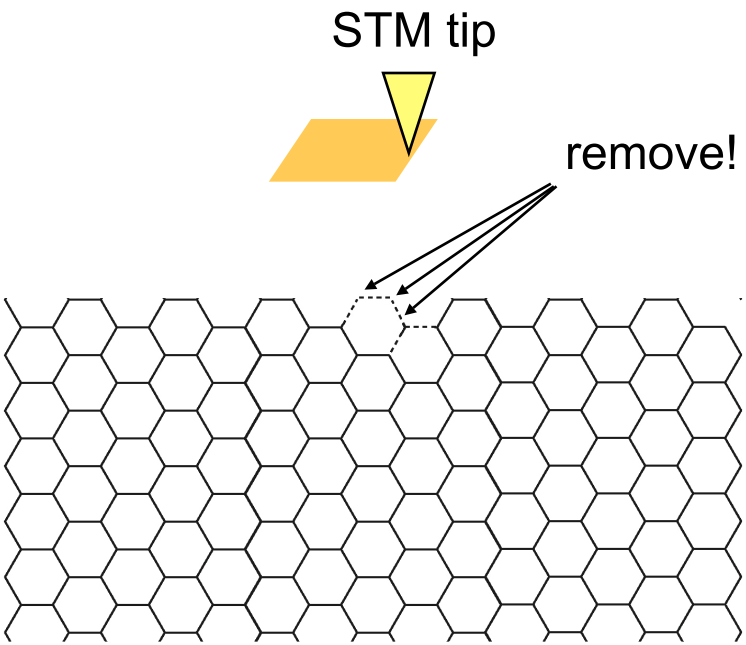

Defective armchair ribbons

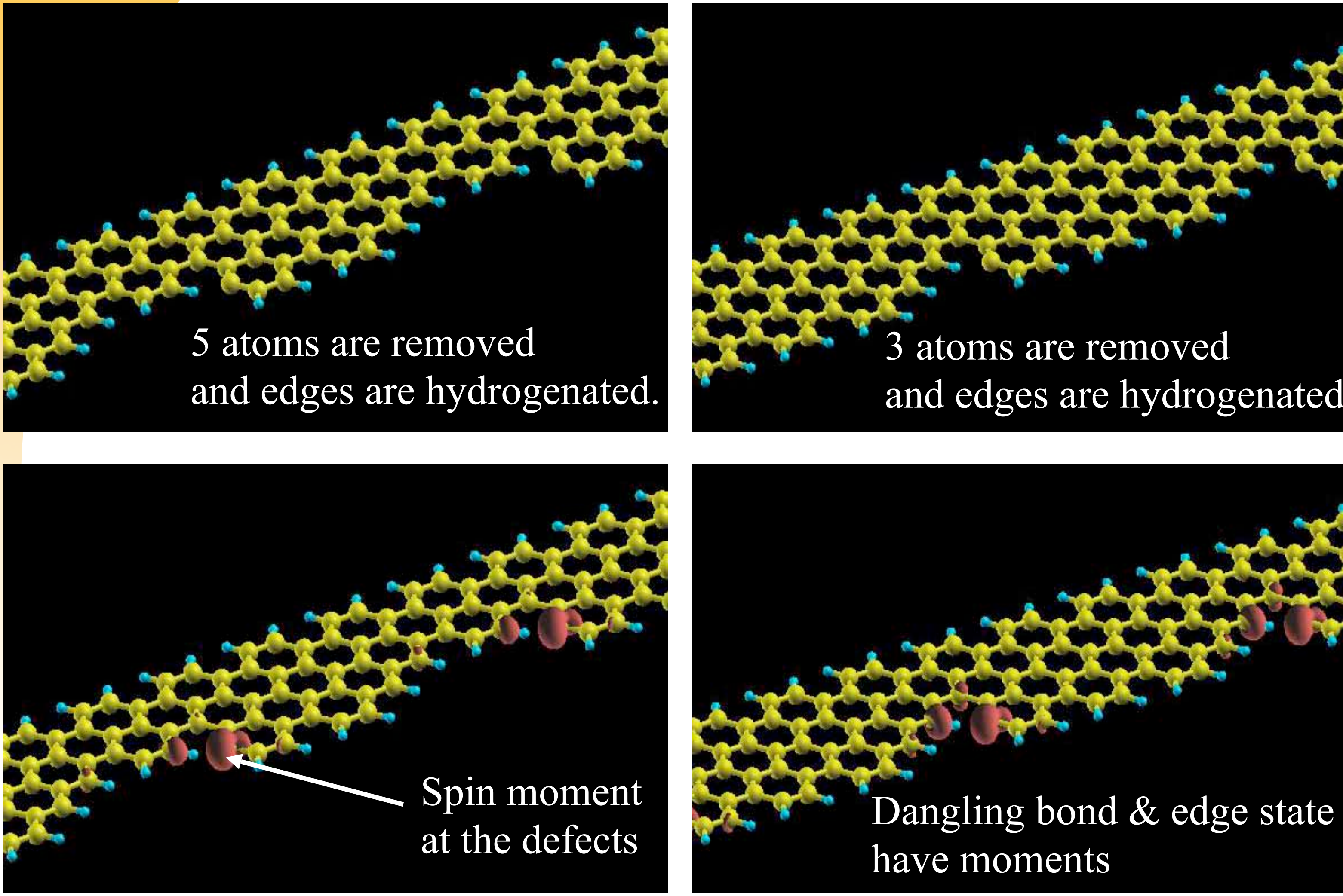

K. Kusakabe, Multifunctional Conducting Molecular Materials, Edt. Gunji Saito et al. (RSC Publishing, 2006), 232-236. .

Defective armchair ribbons

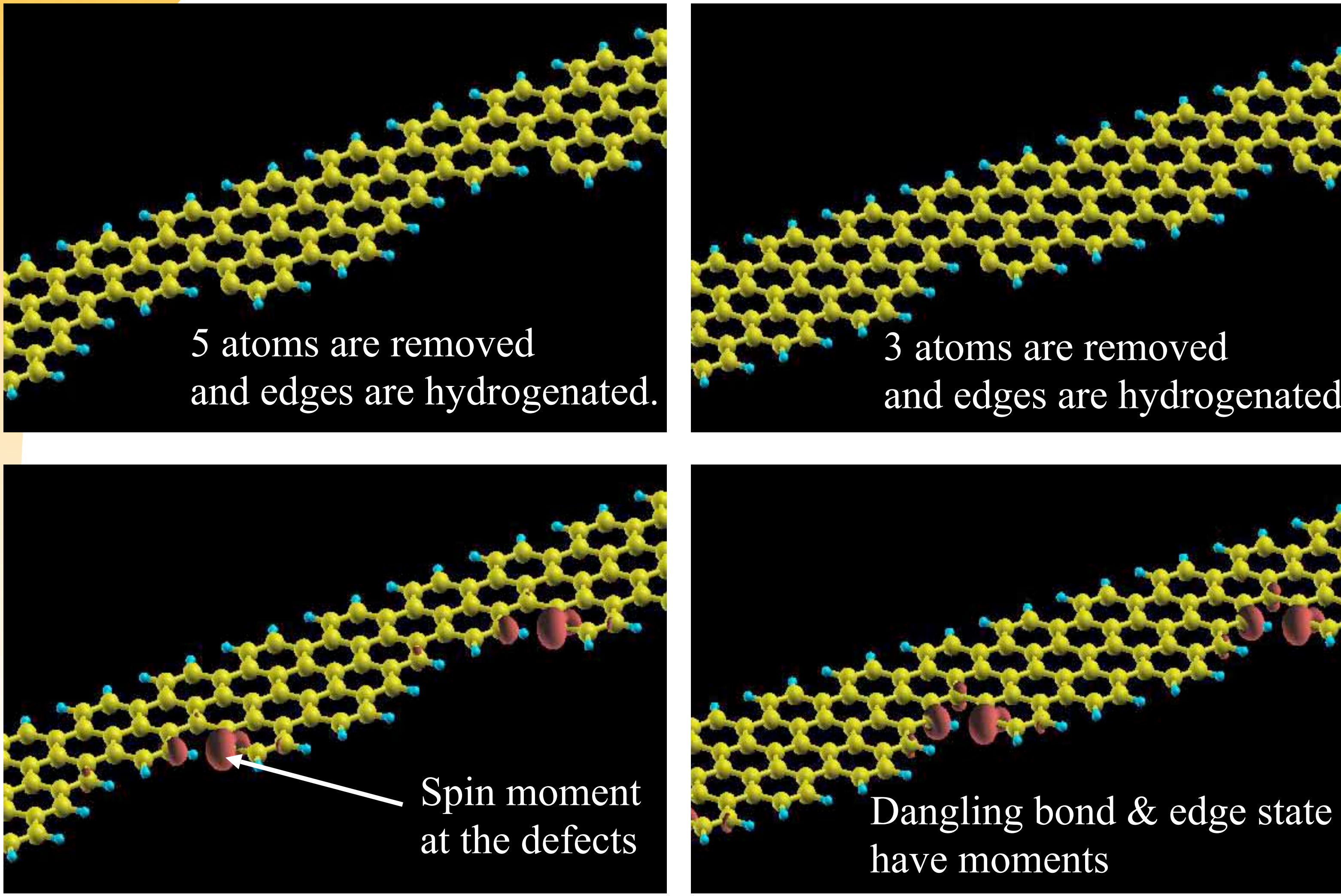

K. Kusakabe, Multifunctional Conducting Molecular Materials, Edt. Gunji Saito et al. (RSC Publishing, 2006), 232-236. .

Defective armchair ribbons

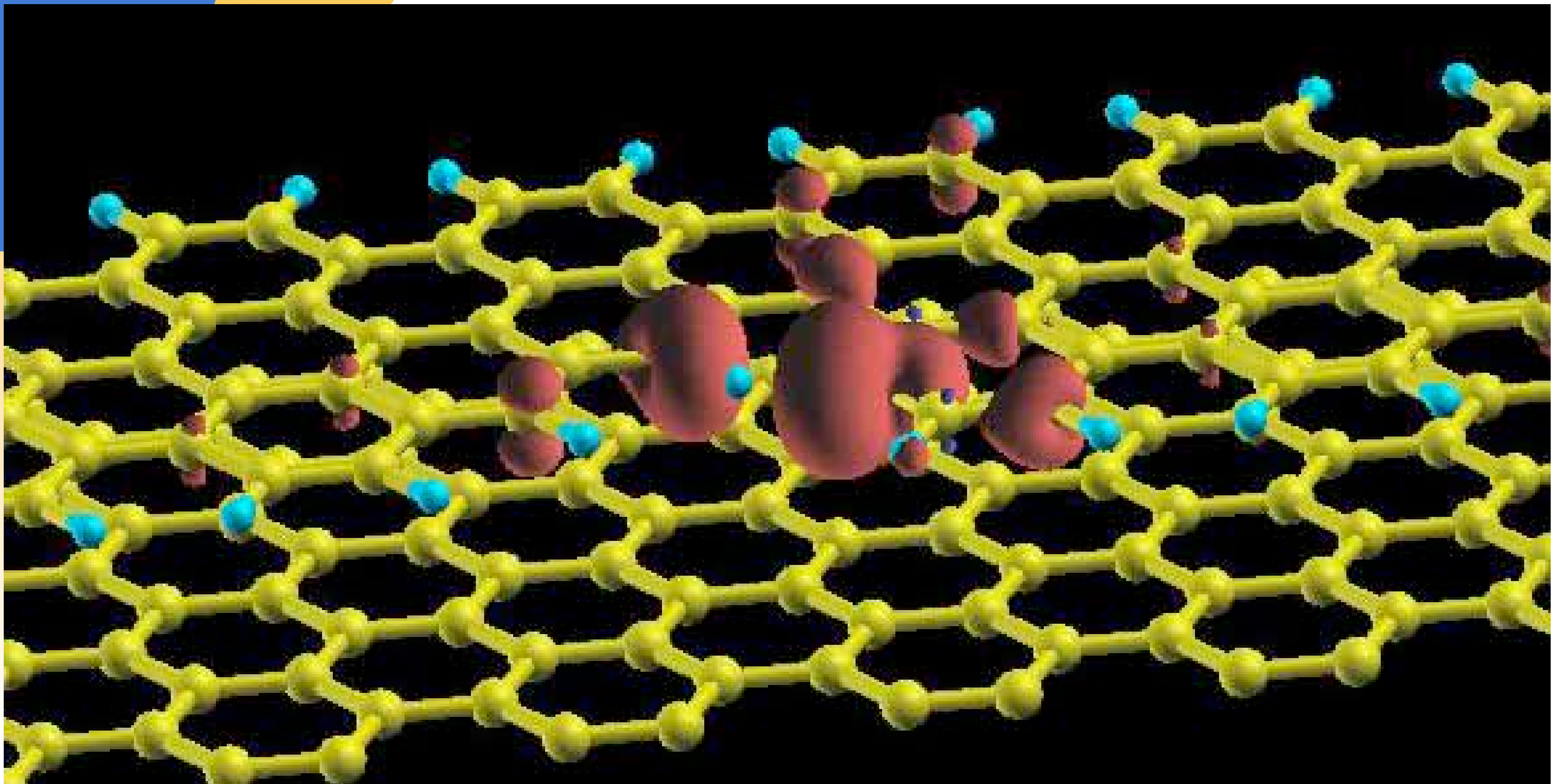

A magnetic graphene ribbon may be created on the graphite surface.

K. Kusakabe, Multifunctional Conducting Molecular Materials, Edt. Gunji Saito et al. (RSC Publishing, 2006), 232-236. .

Effects of Fe impurities

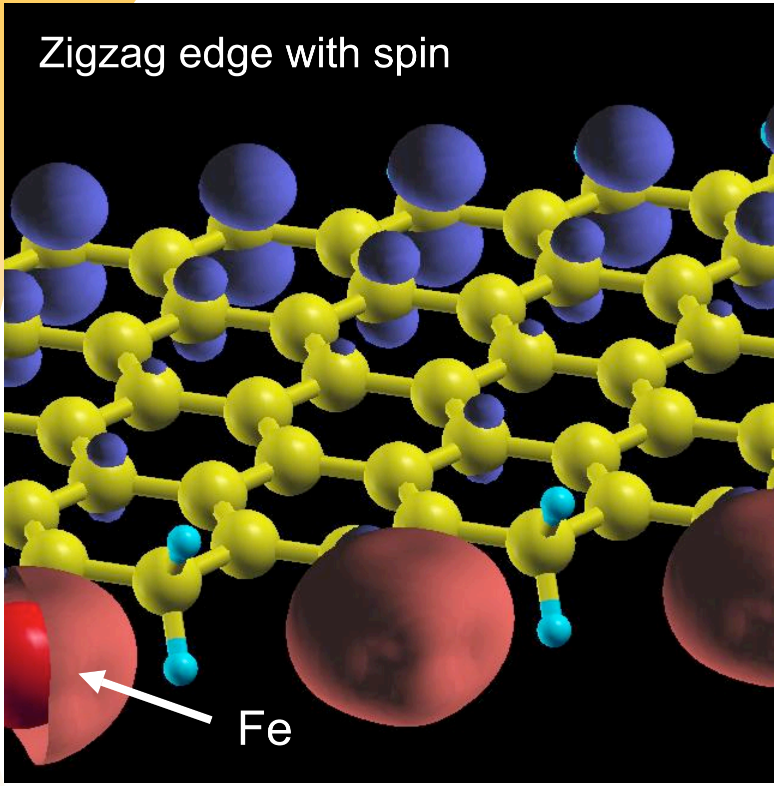

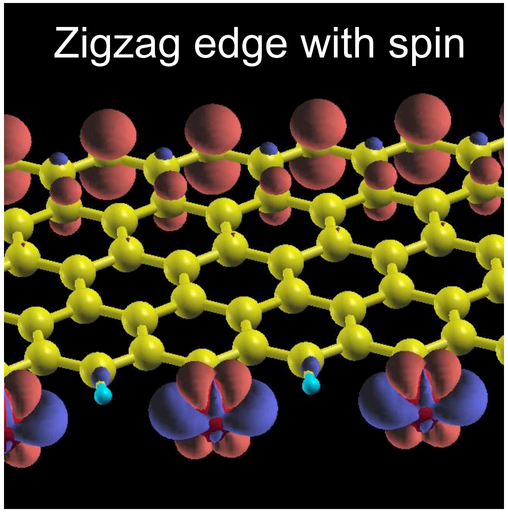

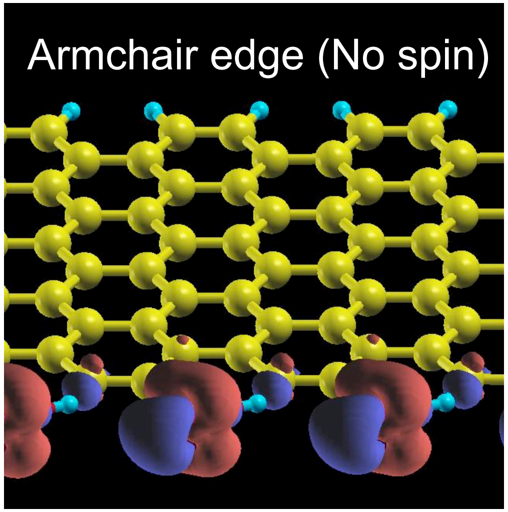

Fe impurity does not necessarily induce magnetic moments in graphene structure. But, the zigzag edge has moments.

Effects of Fe impurities

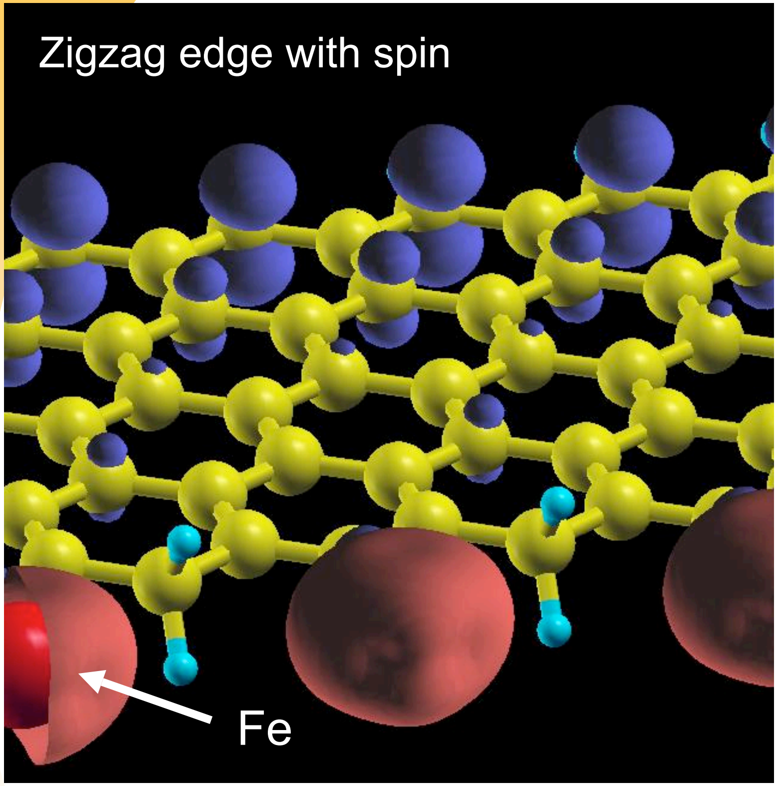

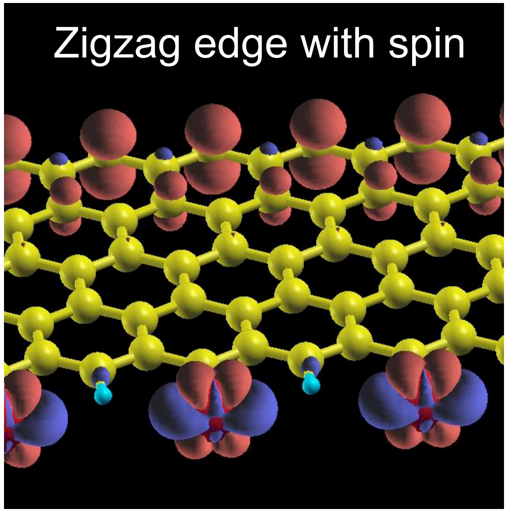

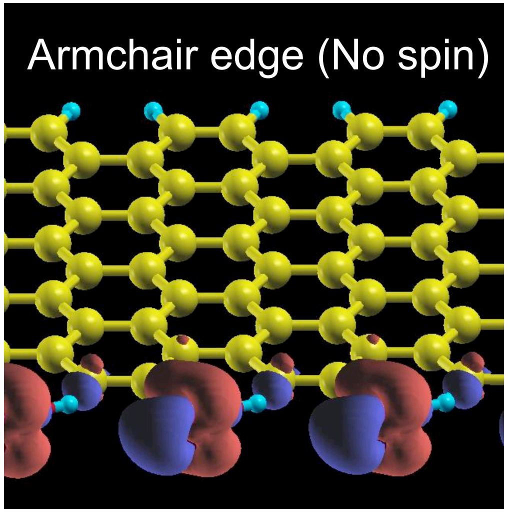

Fe impurity does not necessarily induce magnetic moments in graphene structure. But, the zigzag edge has moments.

Osaka Univ.
CMD®

Graphene/Ni(111)

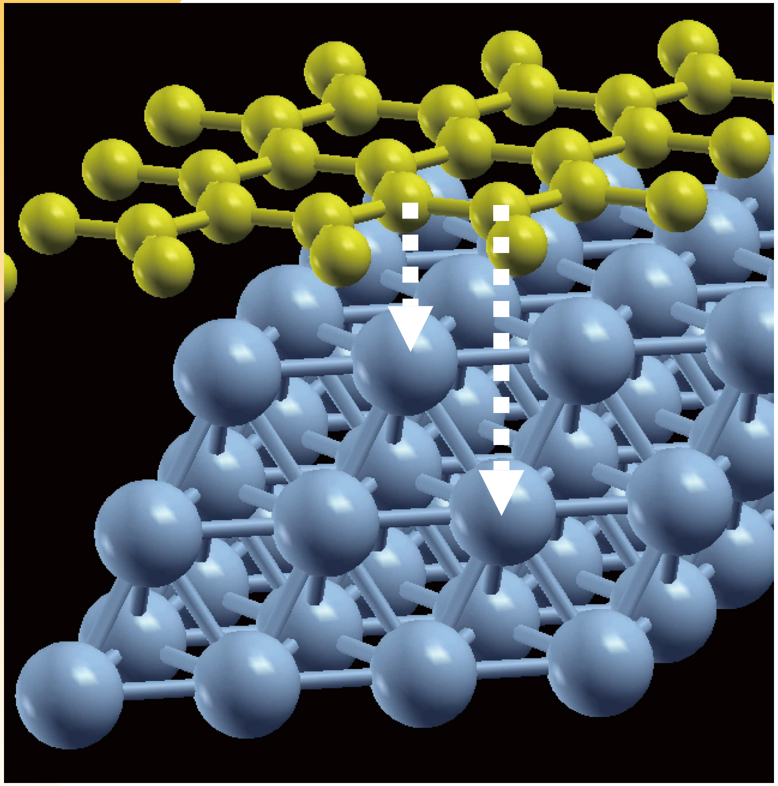

Model B

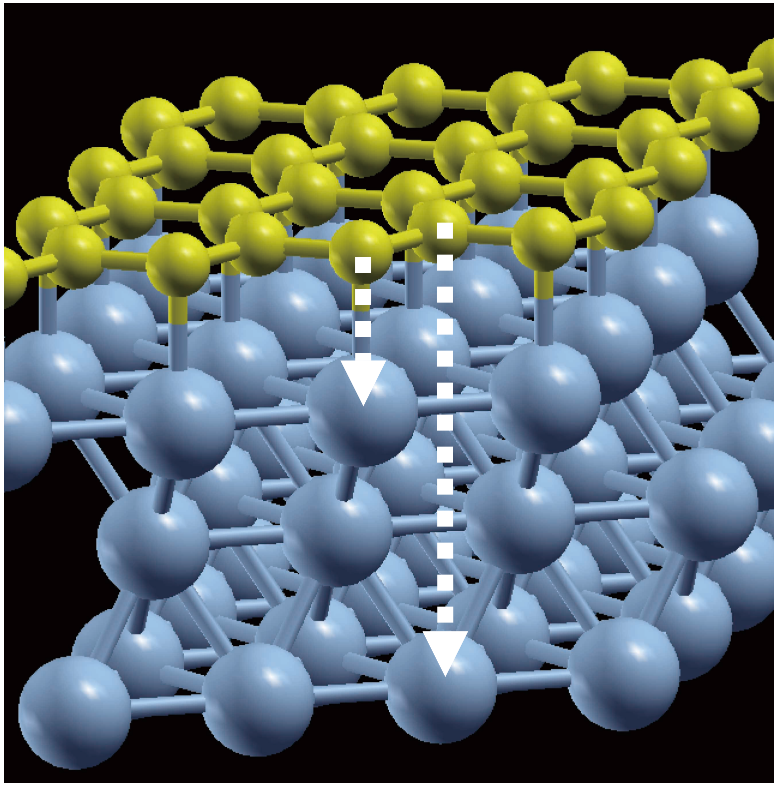

Model C

For both models, the majority band has a slightly filled upper π branch, and the minority band has a filled lower π branch at K.

Cf. G. Bertoni, et al. Phys. Rev. B 71 (2004) 075502.

Graphene/Ni(111)

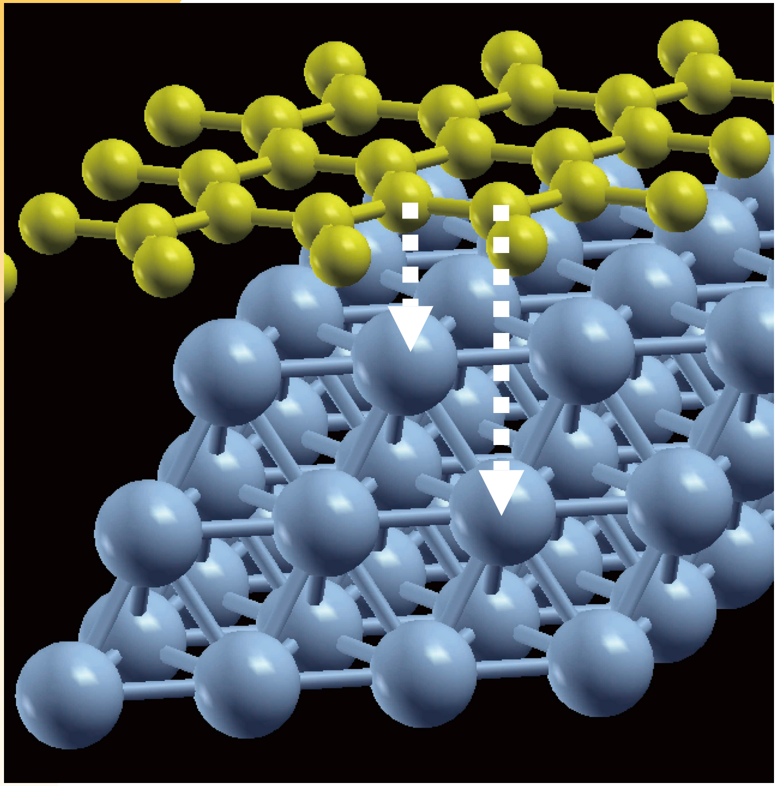

Model B

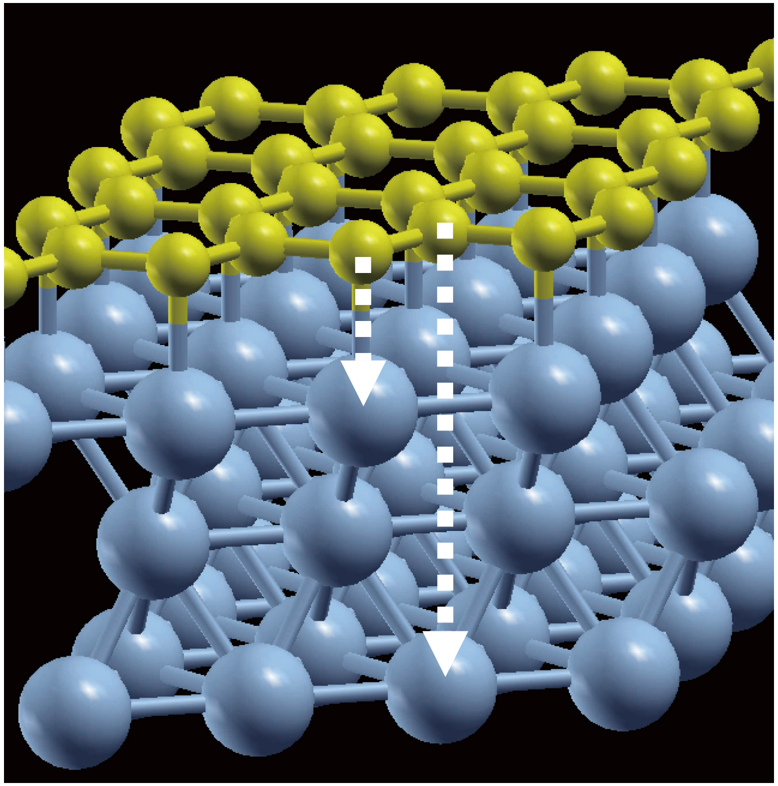

Model C

For both models, the majority band has a slightly filled upper π branch, and the minority band has a filled lower π branch at K.

Cf. G. Bertoni, et al. Phys. Rev. B 71 (2004) 075502.

Calculation conditions

- **The plane-wave expansion method with the ultra-soft pseudo-potentials for C & Ni.**
- **GGA by PBE96.**
- **Energy cut-off : 25Ry for wf, 150Ry for charge.**
- **8x8x1 k-mesh for graphene/Ni(111) interface, 8x1x1 k-mesh for graphene with a Ni bar.**
- **The vacuum layer : 10 a.u. width.**
- **The Quantum-espresso ver 3.2.2 is utilized,**

Calculation conditions

- **The plane-wave expansion method with the ultra-soft pseudo-potentials for C & Ni.**
- **GGA by PBE96.**
- **Energy cut-off : 25Ry for wf, 150Ry for charge.**
- **8x8x1 k-mesh for graphene/Ni(111) interface, 8x1x1 k-mesh for graphene with a Ni bar.**
- **The vacuum layer : 10 a.u. width.**
- **The Quantum-espresso ver 3.2.2 is utilized,**

Band structure of graphene/Ni(111)

Minority band

Majority band

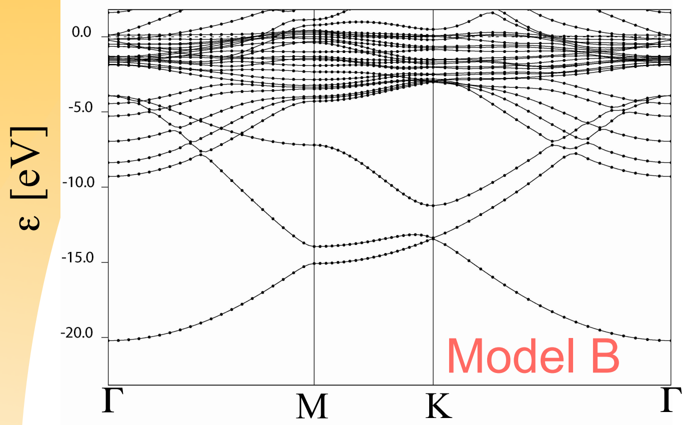

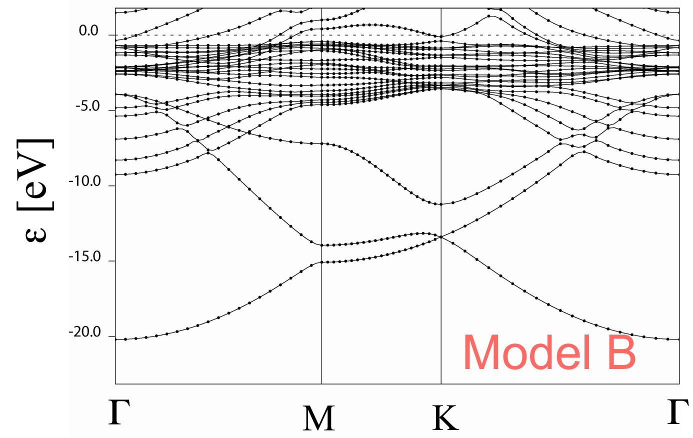

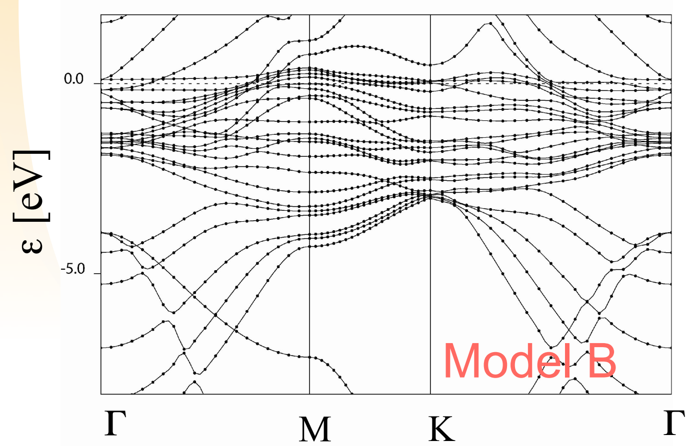

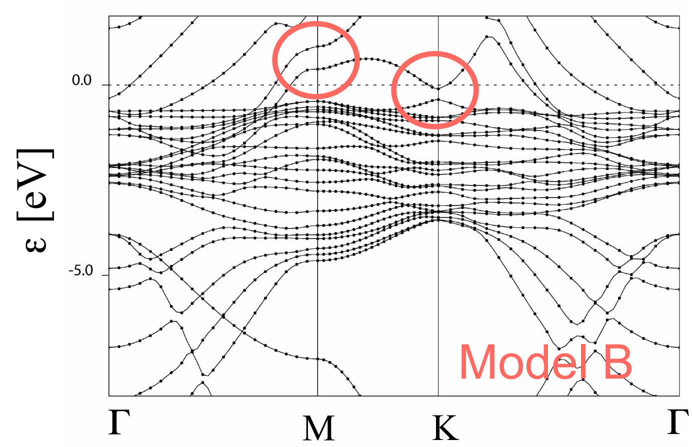

Band structure of graphene/Ni(111)

Minority band	Majority band

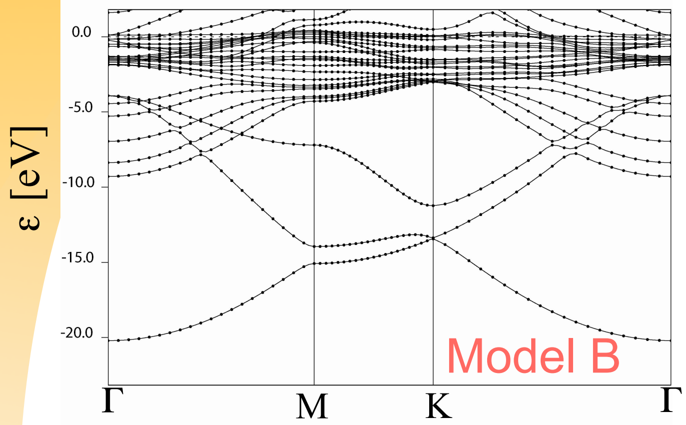

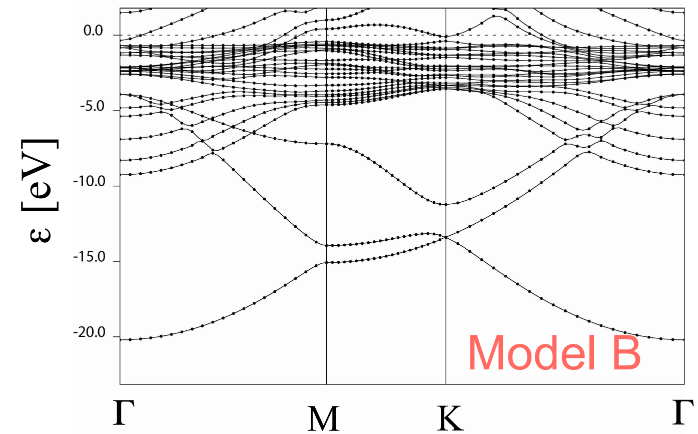

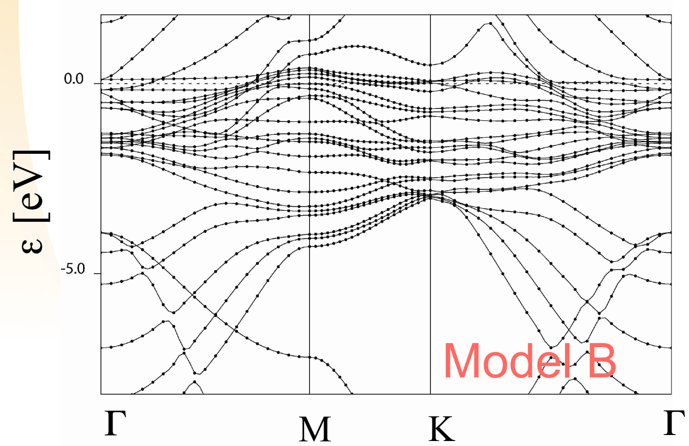

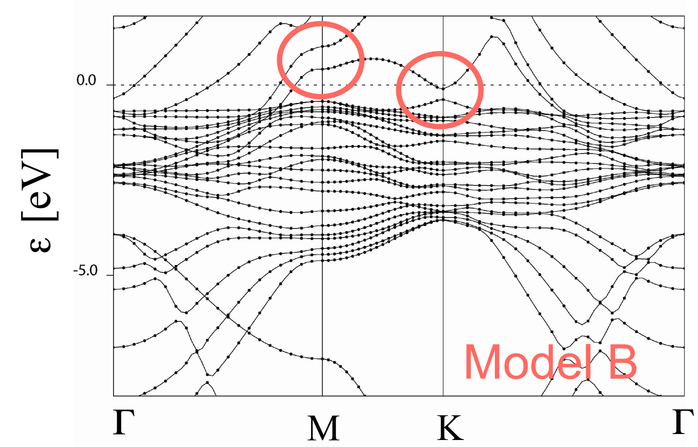

Band structure of graphene/Ni(111)

- The systems are spin polarized.
- For the model B and C, the π band has a gap at the K point.
- The majority π band has a small electron pocket at K. The minority π band is embeded in Ni d bands.
- For the model B, the p-d mixed majorith branch is well above the Fermi level. But, it goes down to the Fermi level in the stable model C.

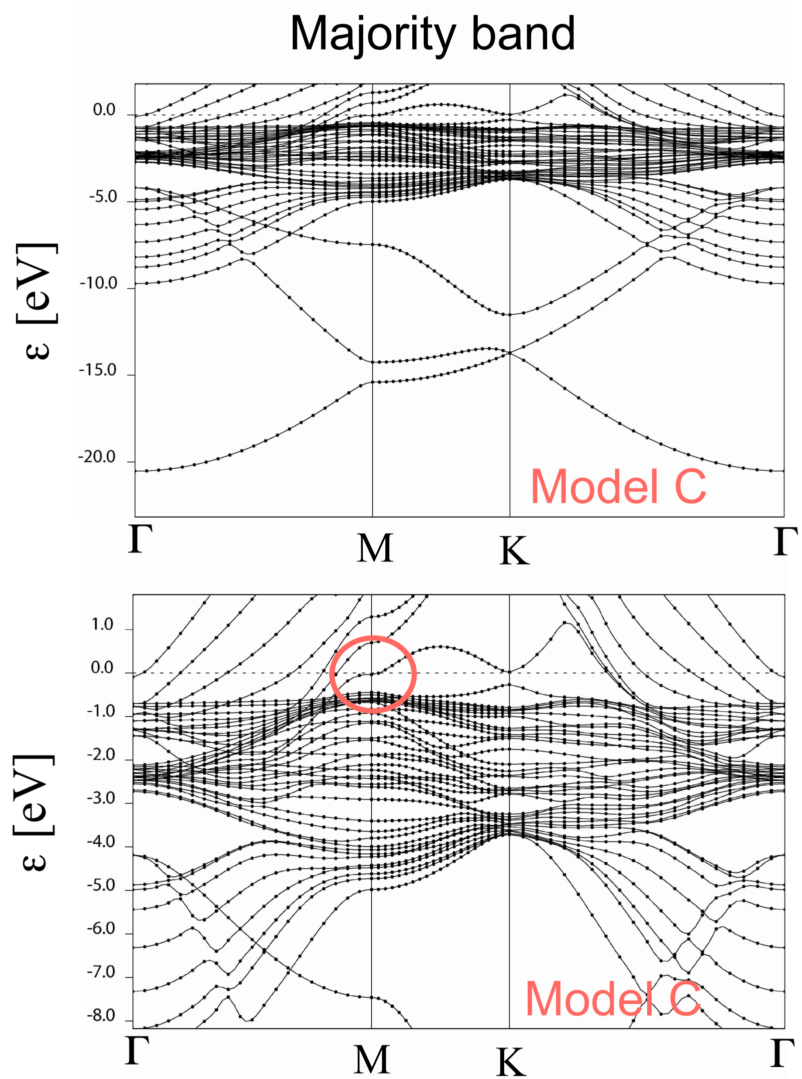

Osaka Univ.
CMD®

Band structure of graphene/Ni(111)

- The systems are spin polarized.
- For the model B and C, the π band has a gap at the K point.
- The majority π band has a small electron pocket at K. The minority π band is embeded in Ni d bands.
- For the model B, the p-d mixed majorith branch is well above the Fermi level. But, it goes down to the Fermi level in the stable model C.

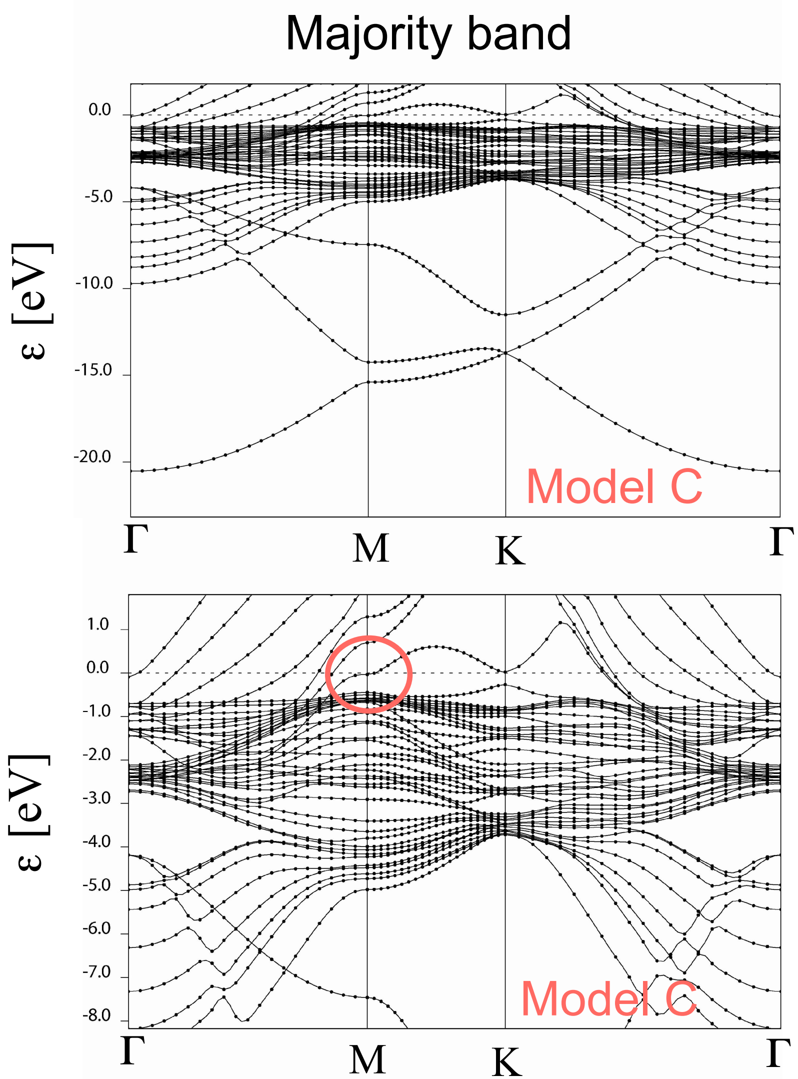

A graphene/Ni junction structure

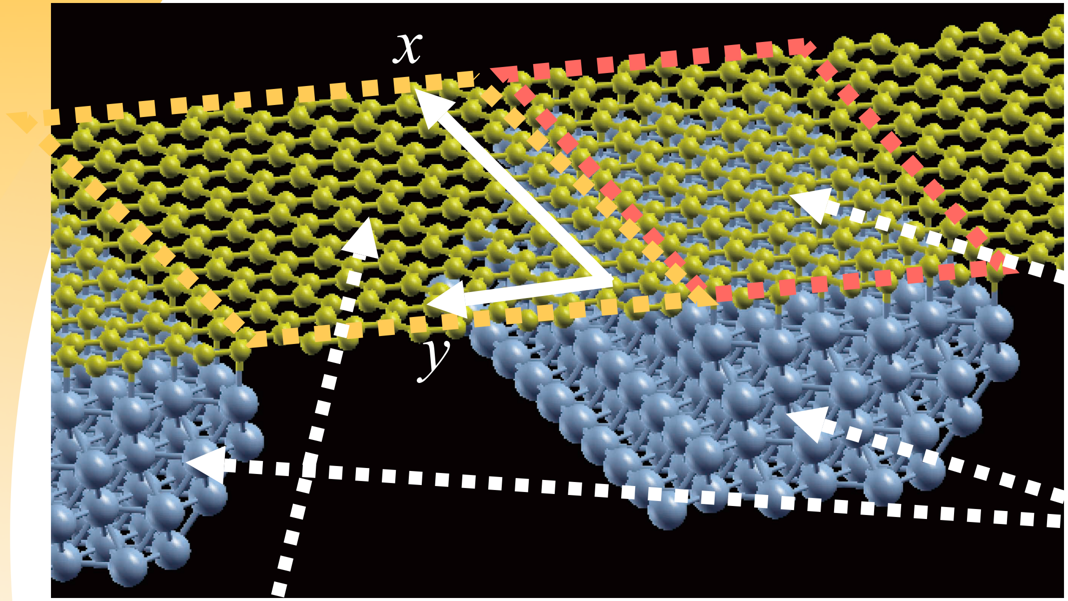

Gapped graphene
(Gap at the K points)

Magnetic electrode

Metallic graphene

A MM/G/M/G/MM junction (M: metal, G: Gapped, MM: magnetic metal)

Theoretical clues to understand its nature:

1. The LDA band structure loses dispersion in the *y* direction around E_F.
2. Gapped graphene is formed by potential due to the Ni substrate.

A graphene/Ni junction structure

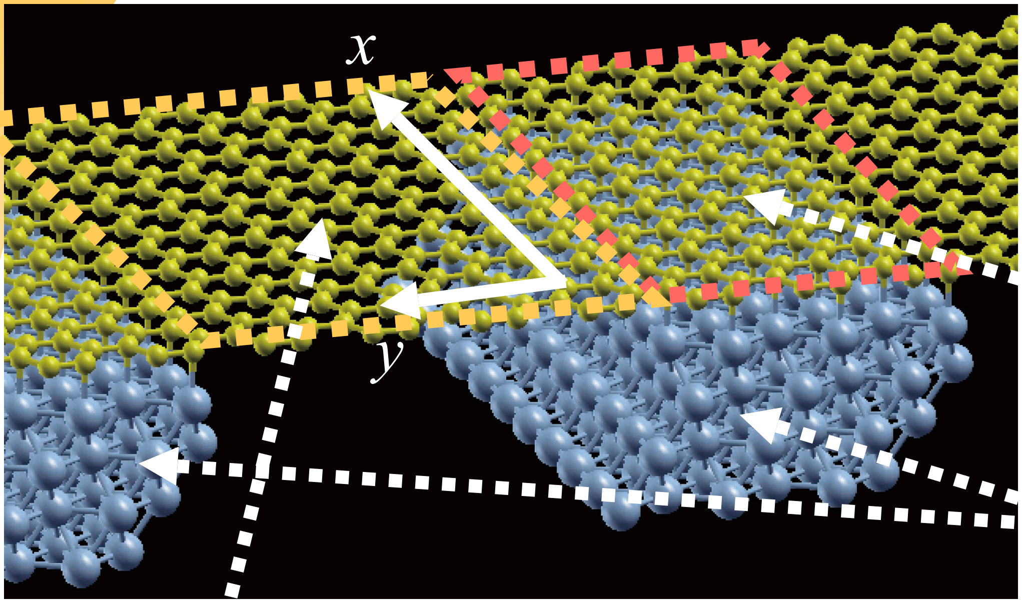

Gapped graphene
(Gap at the K points)

Magnetic electrode

Metallic graphene

A MM/G/M/G/MM junction (M: metal, G: Gapped, MM: magnetic metal)

Theoretical clues to understand its nature:

1. The LDA band structure loses dispersion in the *y* direction around E_F.
2. Gapped graphene is formed by potential due to the Ni substrate.

Two edge structures

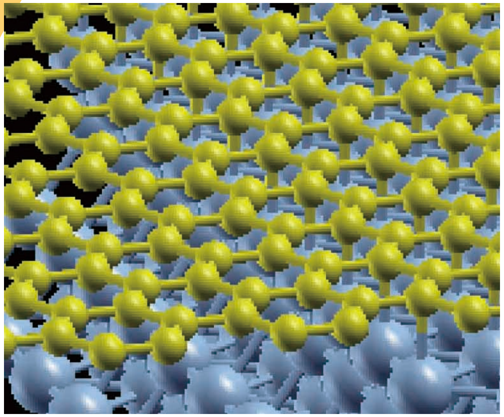

A zigzag edge

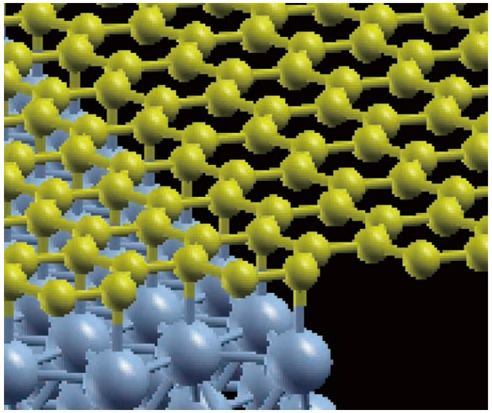

Klein's edge

- **In a tight binding description, Ni atoms produce site-selective potential, which appears as a diagonal (flavor dependent) potential to the two-dimensional Dirac fields.**
- **We would have two different edge structures of interfaces, a zigzag and Klein's edges, between graphene and Ni electrodes.**
- **Thus, we have a room to have a finite graphene ribbon in between two Ni electrodes.**

Two edge structures

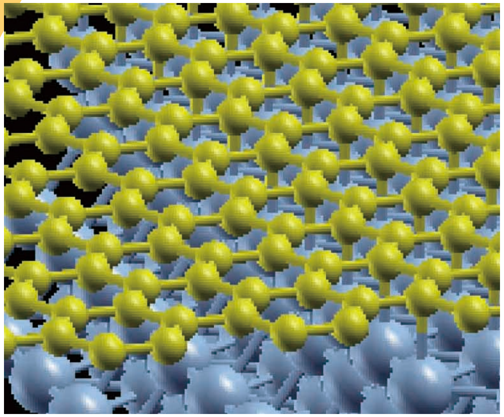

A zigzag edge

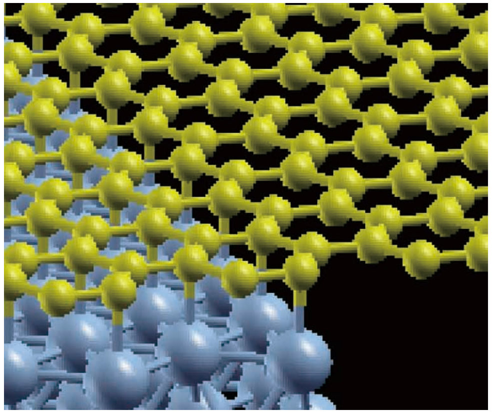

Klein's edge

- **In a tight binding description, Ni atoms produce site-selective potential, which appears as a diagonal (flavor dependent) potential to the two-dimensional Dirac fields.**
- **We would have two different edge structures of interfaces, a zigzag and Klein's edges, between graphene and Ni electrodes.**
- **Thus, we have a room to have a finite graphene ribbon in between two Ni electrodes.**

Band structure of monolayer graphene

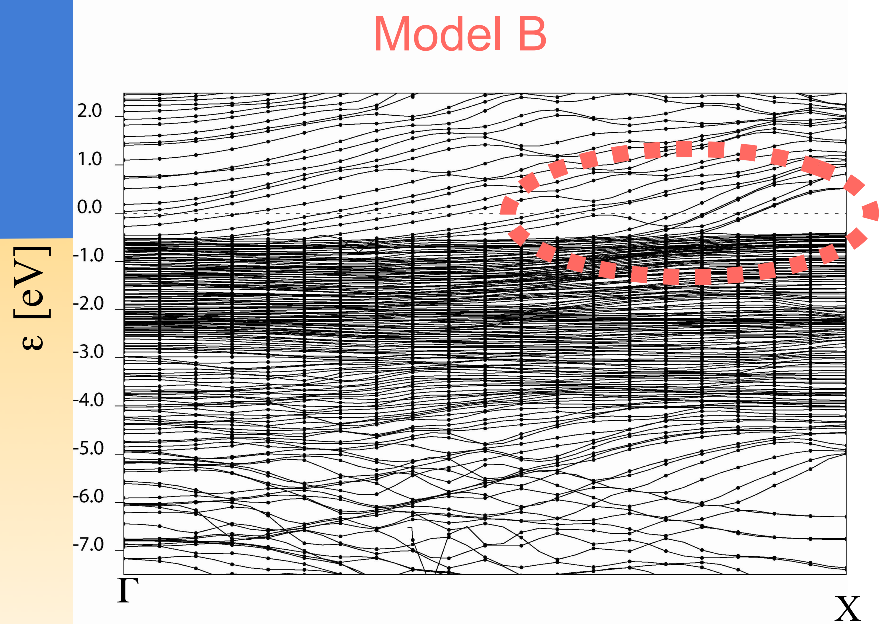

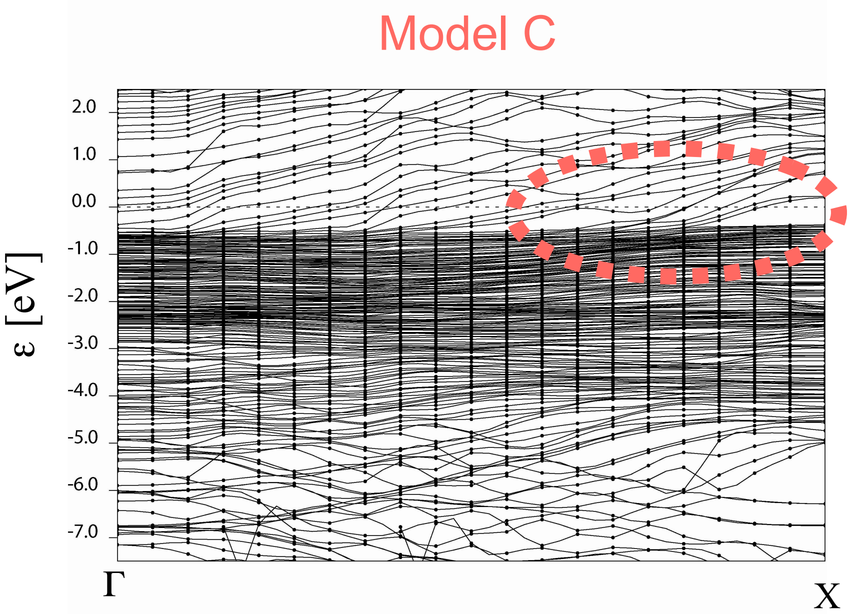

- **These are non-magnetic solutions, although the starting magnetization is finite for this spin-GGA calculation.**
- **Dispersion relation around the X point suggests that π character remains in the electronic state.**
- **To construct an effective theory for this structure, modeling of d orbital as well as π orbital should be demanded.**

Osaka Univ.
CMD®

Band structure of monolayer graphene

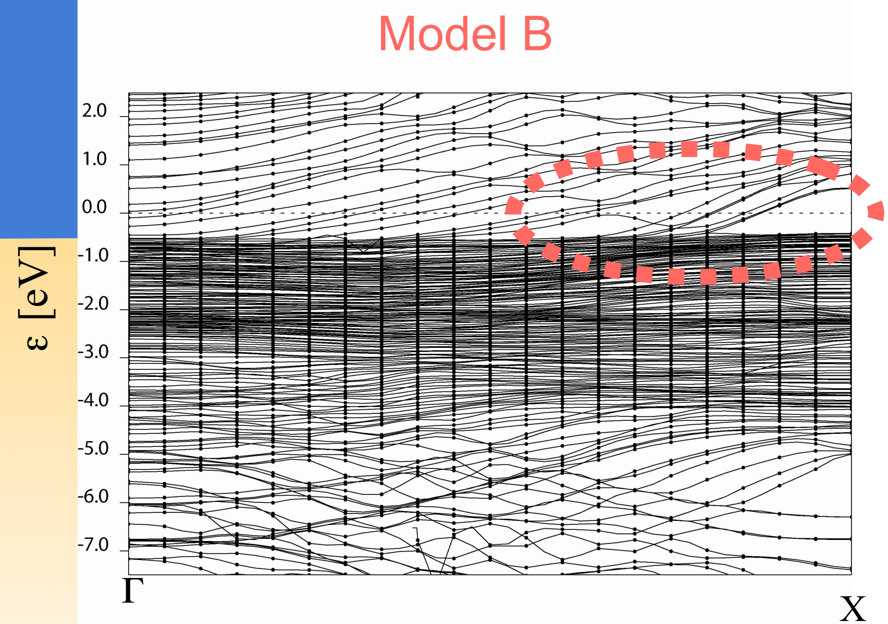

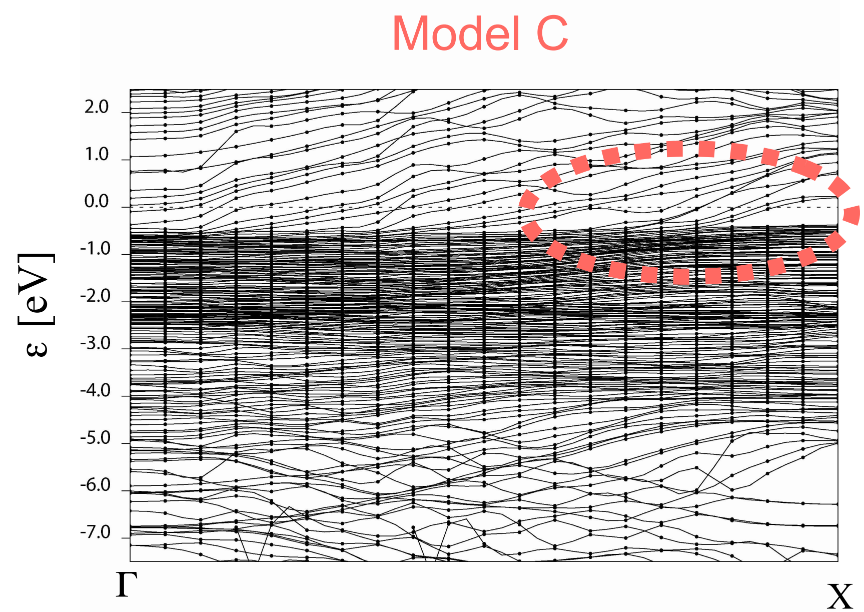

- **These are non-magnetic solutions, although the starting magnetization is finite for this spin-GGA calculation.**
- **Dispersion relation around the X point suggests that π character remains in the electronic state.**
- **To construct an effective theory for this structure, modeling of d orbital as well as π orbital should be demanded.**

Possible device structures

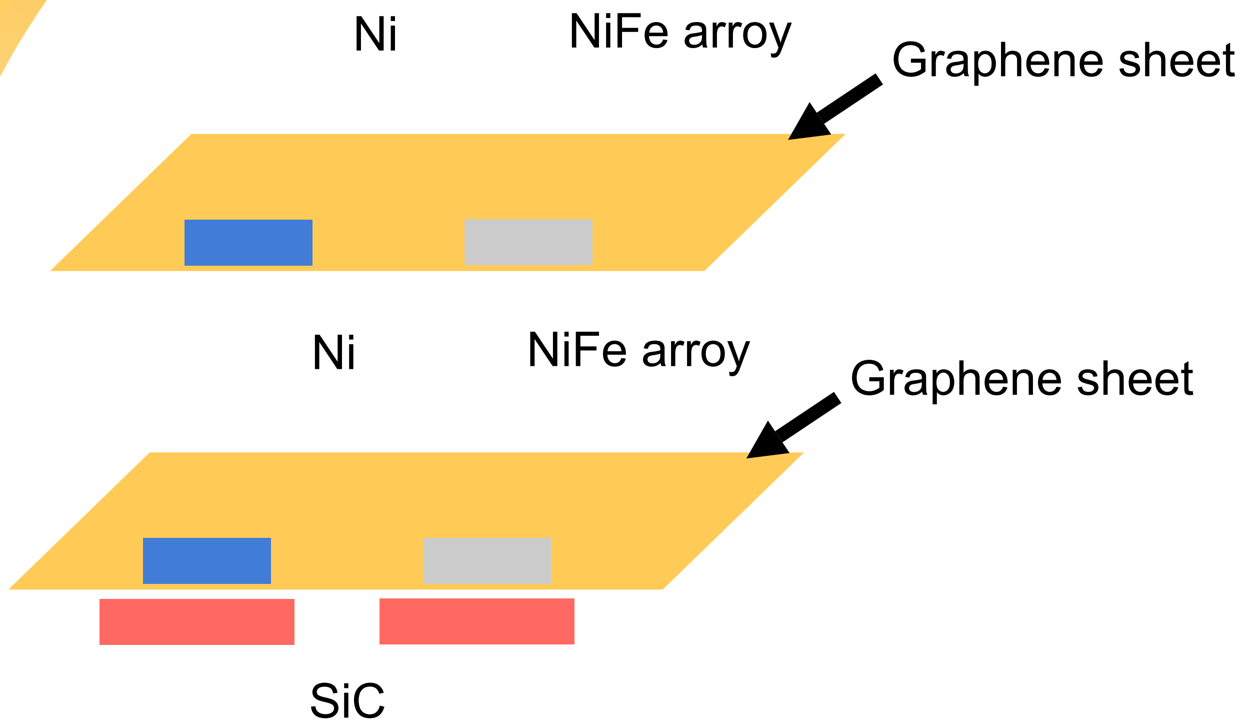

Comments:

1. To aboid undesired direct current flow from magnetic electrodes to graphene we may utilize SiC to induce alternating potential to make a gap in graphene.
2. The spin-orbit interaction may be enhanced in the π electron system, if the single-layered graphene is placed undere an non-symmetric environment, e.g. on a metallic substrate.

Possible device structures

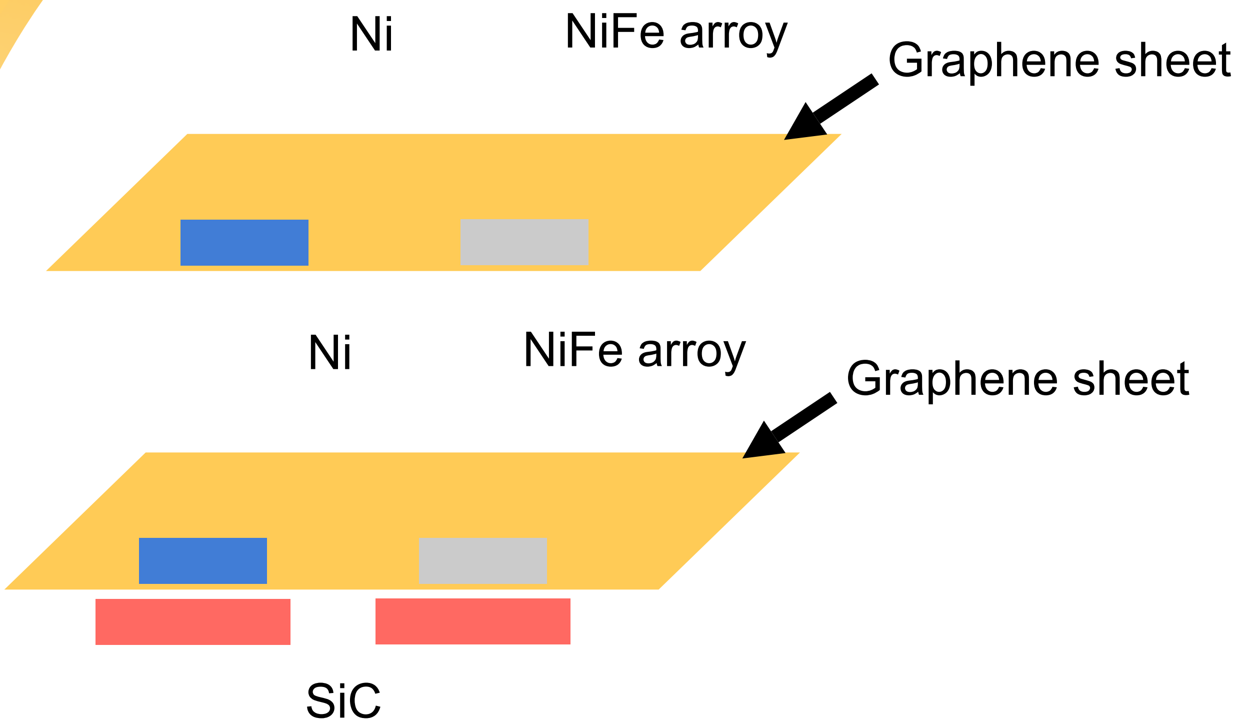

Comments:

1. To aboid undesired direct current flow from magnetic electrodes to graphene we may utilize SiC to induce alternating potential to make a gap in graphene.
2. The spin-orbit interaction may be enhanced in the π electron system, if the single-layered graphene is placed undere an non-symmetric environment, e.g. on a metallic substrate.

Summary

Summary

Summary

- **We have designed magnetic nano-graphite structures,**
  - Magnetic nano-graphene including wires and molecules,
  - Magnetic nano-wire on a diamond surface.

Summary

- **We have designed magnetic nano-graphite structures,**
  - Magnetic nano-graphene including wires and molecules,
  - Magnetic nano-wire on a diamond surface.
- **LSDA (or GGA) calculations conclude magnetic structures. The result is consistent with expectation obtained by consideration of the Hubbard model.**

Summary

- **We have designed magnetic nano-graphite structures,**
  - Magnetic nano-graphene including wires and molecules,
  - Magnetic nano-wire on a diamond surface.
- **LSDA (or GGA) calculations conclude magnetic structures. The result is consistent with expectation obtained by consideration of the Hubbard model.**
- **Possible device structures are proposed utilizing interfaces between graphene and the Ni (111) surface.**

Summary

- **We have designed magnetic nano-graphite structures,**
  - Magnetic nano-graphene including wires and molecules,
  - Magnetic nano-wire on a diamond surface.
- **LSDA (or GGA) calculations conclude magnetic structures. The result is consistent with expectation obtained by consideration of the Hubbard model.**
- **Possible device structures are proposed utilizing interfaces between graphene and the Ni (111) surface.**
- **All the available consideration using various electron models conclude existence of localized magnetism at the zigzag edges of finite graphene ribbon structures.**

Design of Models of Magnetic Materials

- **Present DFT approach : Magnetism by LSDA**
  - Design of magnetic materials using the Heisenberg model, the Hubbard model, etc.
  - Confirm the magnetic solution using the first-principles calculation

- **MR-DFT approach : Magnetism in many-body theory**
  - Design of magnetic materials directly using a correlated electron model from the first principles.
  - Direct simulation of functionality from the first principles: The quantum simulator.
  - A self-consistent electronic structure calculation with interacting electron description enables us to predict functional materials with magnetism.

Design of Models of Magnetic Materials

- **Present DFT approach : Magnetism by LSDA**
  - Design of magnetic materials using the Heisenberg model, the Hubbard model, etc.
  - Confirm the magnetic solution using the first-principles calculation

- **MR-DFT approach : Magnetism in many-body theory**
  - Design of magnetic materials directly using a correlated electron model from the first principles.
  - Direct simulation of functionality from the first principles: The quantum simulator.
  - A self-consistent electronic structure calculation with interacting electron description enables us to predict functional materials with magnetism.

A conclusion from MR-DFT

The Levy-Lieb energy functional is defined by,

$$F[n] = \min_{\Psi \to n} \langle \Psi | \hat{T} + \hat{V}_{ee} | \Psi \rangle.$$

Since $F[n]$ is not a convex functional, it is impossible to have a functional derivative of $F[n]$ w.r.t. $n(\mathbf{r})$. To have a well-defined derivative, we may consider the Lieb functional which is a Legendre transform of $F[n]$. There are several expressions as follows.

$$\begin{aligned}
\bar{F}[n] &= \sup_{v \in L^{3/2}+L^\infty} \left[\inf_{n' \in \mathcal{I}_N} \left\{ \min_{\Psi \to n'} \langle \Psi | \hat{T} + \hat{V}_{ee} | \Psi \rangle + \int d^3r v(\mathbf{r}) n'(\mathbf{r}) \right\} \right. \\
&\quad \left. - \int d^3r v(\mathbf{r}) n(\mathbf{r}) \right], \\
&= \inf_{\hat{D} \to n} \mathrm{tr} \hat{D} (\hat{T} + \hat{V}_{ee}), \\
&= \sup_{v \in L^{3/2}+L^\infty} \left[\min_{\Psi} \langle \Psi | \hat{T} + \hat{V}_{ee} + \int d^3r v(\mathbf{r}) (\hat{n}(\mathbf{r}) - n(\mathbf{r})) | \Psi \rangle \right].
\end{aligned}$$

Quantum mechanics driven by $n(\mathbf{r})$.

Thus we can design future first-principles calculation methods starting from MR-DFT.

A conclusion from MR-DFT

The Levy-Lieb energy functional is defined by,

$$F[n] = \min_{\Psi \to n} \langle \Psi | \hat{T} + \hat{V}_{ee} | \Psi \rangle.$$

Since $F[n]$ is not a convex functional, it is impossible to have a functional derivative of $F[n]$ w.r.t. $n(\mathbf{r})$. To have a well-defined derivative, we may consider the Lieb functional which is a Legendre transform of $F[n]$. There are several expressions as follows.

$$\begin{aligned} \bar{F}[n] &= \sup_{v \in L^{3/2}+L^\infty} \left[\inf_{n' \in \mathcal{I}_N} \left\{ \min_{\Psi \to n'} \langle \Psi | \hat{T} + \hat{V}_{ee} | \Psi \rangle + \int d^3r v(\mathbf{r}) n'(\mathbf{r}) \right\} \right. \\ &\quad \left. - \int d^3r v(\mathbf{r}) n(\mathbf{r}) \right], \\ &= \inf_{\hat{D} \to n} \mathrm{tr} \hat{D} (\hat{T} + \hat{V}_{ee}), \\ &= \sup_{v \in L^{3/2}+L^\infty} \left[\min_{\Psi} \langle \Psi | \hat{T} + \hat{V}_{ee} + \int d^3r v(\mathbf{r}) (\hat{n}(\mathbf{r}) - n(\mathbf{r})) | \Psi \rangle \right]. \end{aligned}$$

Quantum mechanics driven by $n(\mathbf{r})$.

Thus we can design future first-principles calculation methods starting from MR-DFT.